N 72-13046
NASA CR-112002

DEVELOPMENT OF LIGHTWEIGHT ALUMINUM HOLLOWCORE SOLAR CELL ARRAY TECHNOLOGY

By J. A. Carlson

Prepared under Contract No. NAS1-9495 by
ELECTRO-OPTICAL SYSTEMS
Pasadena, California

for

NATIONAL AERONAUTICS AND SPACE ADMINISTRATION

NASA CR-112002

DEVELOPMENT OF LIGHTWEIGHT ALUMINUM HOLLOWCORE SOLAR CELL ARRAY TECHNOLOGY

By J. A. Carlson

Prepared under Contract No. NAS1-9495 by
ELECTRO-OPTICAL SYSTEMS
Pasadena, California

for

NATIONAL AERONAUTICS AND SPACE ADMINISTRATION

Page intentionally left blank

SUMMARY

The primary objective of the program was to develop and demonstrate the technology required for fabrication of a lightweight-deployable solar cell array. A baseline configuration for a three section folding array, with retraction capability, was developed which would utilize electroformed aluminum hollowcore substrates and beryllium frames. The three section array was not fabricated because of difficulties with impurities in the aluminum electroforming bath. A procedure was developed for etching the copper mandrel from virtually any size of aluminum hollowcore panel in approximately one hour. Procedures were developed for analyzing the content of peroxide, water, total aluminum, and lithium-aluminum-hydride in an aluminum electroforming solution.

Page intentionally left blank

CONTENTS

CONTENTS (Contd)

ILLUSTRATIONS

ILLUSTRATIONS (Contd)

SECTION 1

INTRODUCTION

The primary objective of the program was to develop and demonstrate the technology required for the successful fabrication of a lightweight solar cell array and its integration into a deployable system. The demonstration array was to be a three-section, 75 square foot folding array which would utilize electroformed aluminum hollowcore substrates and beryllium frames. This work was an extension of the technology developed under Contract NAS7-428 and reported in NASA CR-66832, Development of Lightweight Solar Panels.

The work completed during the term of this program and documented in this report includes:

a. Development of the baseline configuration for the three-section deployable array

b. Investigation of the mechanics of array deployment

c. Parametric analysis of allowable loads of curved beams

d. Preliminary definition of procedures for thermal testing task

e. Maintenance and repair of the main plating facility equipment

f. Evaluation of aluminum electro-forming and mandrel etching solutions

g. Analytical and experimental investigation of mandrel materials and dissolution processes

h. Thermal surface property measurements on electroformed aluminum with various surface treatments and on Kapton H-film with simulated solar cell backup

i. Efforts directed toward preparing a 500 gallon batch of new mixed ether aluminum plating solution

j. Effort directed toward obtaining large quantities of aluminum chloride of acceptable purity for this program

k. Developing techniques and procedures for analyzing aluminum plating solutions

l. Fabrication of four beryllium tubes required for assembling the third 5 foot by 5 foot aluminum hollowcore panel

SECTION 2

DESCRIPTION OF PROGRAM TASKS

The program was divided into four major tasks:

a. Mandrel evaluations
b. Electroforming process studies
c. Thermal tests
d. Development of a deployable array

The work included in tasks a through c provided the technology required to achieve the primary objective of the program which was task d, the development of a three-section deployable array. A description of the objectives of each task follows.

2.1 MANDREL EVALUATIONS

a. Determine the optimum conditions for dissolution of a pure copper mandrel from an electroformed aluminum hollowcore
b. Investigate the feasibility of using alternative mandrel materials in the aluminum electroforming process
c. Summarize time/ft^2 and cost/ft^2 for each feasible mandrel material alternative

2.2 ELECTROFORMING PROCESS STUDIES

a. Perform analytical and experimental investigations with the goal of increasing the throwing power of the plating process
b. Investigate the functional relations between the plating parameters and the skin thickness of the finished electroform

2.3 THERMAL TESTS

a. Make absorptivity and emissivity measurements on electroformed aluminum hollowcore specimens with and without thermal coatings

2.4 DEPLOYABLE ARRAY DEVELOPMENT

The objective of this task was to demonstrate the feasibility of using the hollowcore panels in large-area deployable arrays. The program design criteria and requirements to be met in this task were those given in Chapter 2 of NASA CR-75370, Development of Lightweight Rigid Solar Panel, Interim Design Report, EOS Report 7027-IDR. Where applicable, the results of the tasks described in subsections 2.1 through 2.3 were used in performance of this task.

a. Design a deployable array consisting of three 5 foot by 5 foot panels utilizing electroformed aluminum, biconvex, hollowcore substrates and beryllium frames.

b. Design the required mechanisms for deployment and latching of the three-panel array. Consideration was given to the problem of refolding the array in flight.

c. Calculate and analyze the thermal and dynamic characteristics of the undeployed and deployed array.

d. Fabricate one hollowcore substrate and the necessary frames, attachment hardware, and mechanisms for an array, as designed in the preceding step a.

   Two panels for the array were fabricated under Contract NAS7-428 and were modified as required for use in the three-panel array.

SECTION 3

MANDREL EVALUATION

An optimization study of the mandrel forming and dissolution processes was performed with an end item goal of minimizing mandrel costs. Primary emphasis was placed on understanding the dissolution phenomenon and optimizing the methodology associated with the copper mandrel-HNO_3 etchant system presently used. Secondary efforts were expended evaluating alternate materials.

3.1 COPPER MANDREL STUDIES

The first step applied was the experimental evaluation of the dissolution rates of copper and aluminum in nitric acid for various acid concentrations and temperatures. The obvious and most desirable result being an acid concentration and temperature that has maximum dissolution effect on the copper mandrel with negligible dissolution of the aluminum. This experimental effort was conducted in four steps, as described below:

3.1.1 DISSOLUTION OF COPPER AND ALUMINUM IN NITRIC ACID

The dissolution rates of copper and aluminum in 50 percent and 70 percent HNO_3 were measured over the temperature range of 25^{o} to $65^{o}C$. The results of these tests are shown in Figs. 1, 2, 3 and 4. The dissolution rate of aluminum in inches per year (ipy) is plotted against temperature in Fig. 1 and against time in Fig. 2. In both figures, the acid attack on the aluminum is more pronounced at the lower concentration. This result is confirmed by data from the literature (Ref. 1) as shown in Fig. 3. The data shown indicates negligible aluminum dissolution at high HNO_3 concentrations increasing markedly as the HNO_3

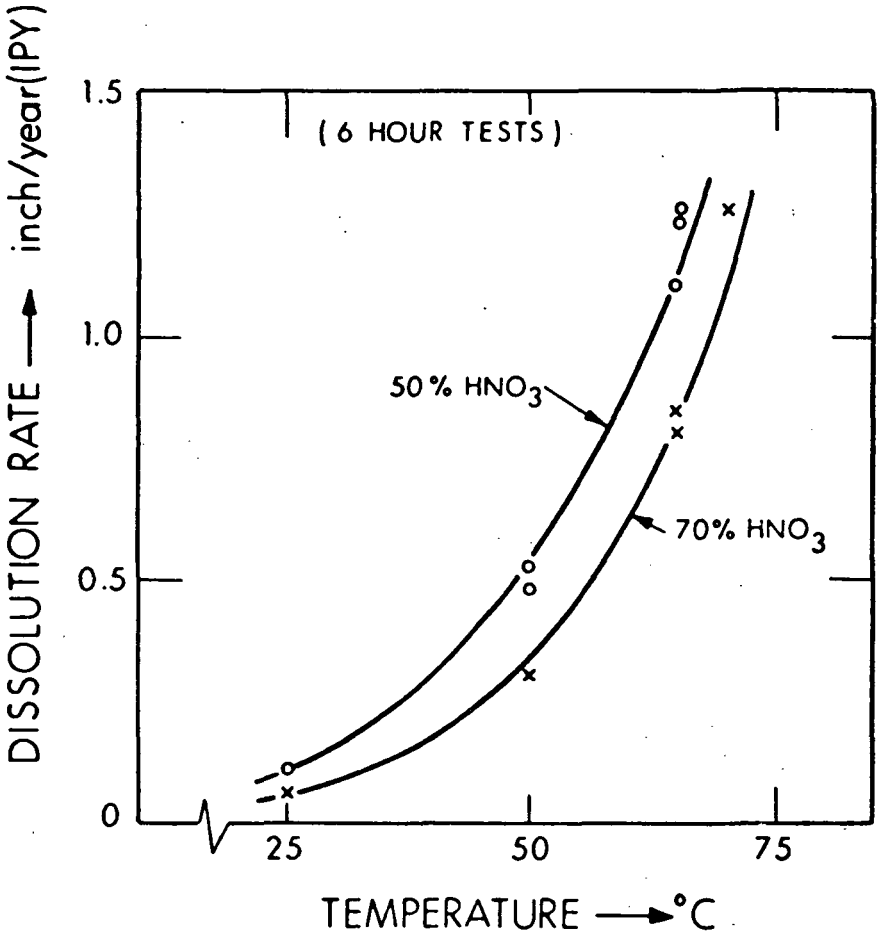

Figure 1. Dissolution Rates of Aluminum in Nitric Acid

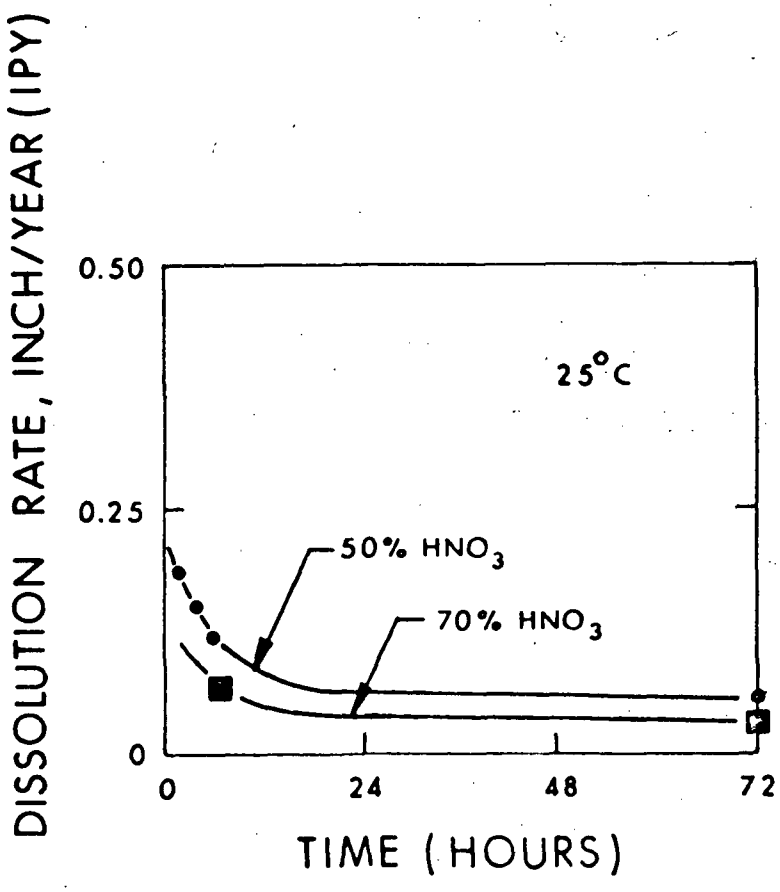

Figure 2. Effect of Exposure Time on Dissolution Rate of Aluminum

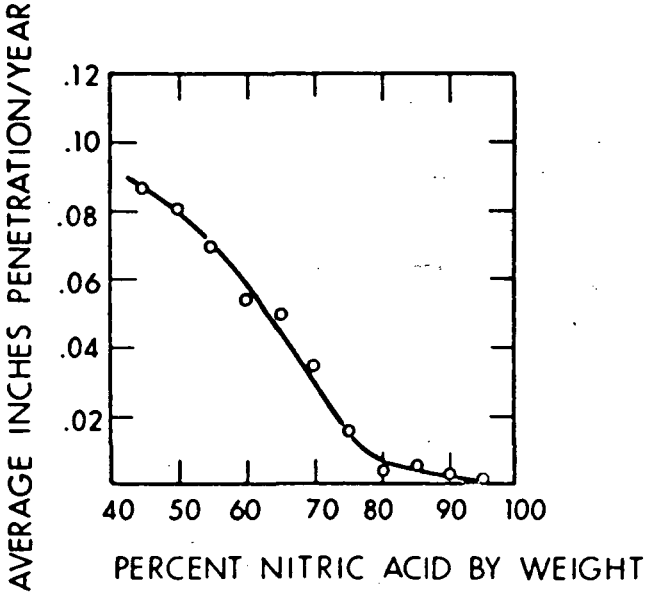

Figure 3. Action of Nitric Acid on 2S-H Aluminum (90-Day Tests, Room Temperature)

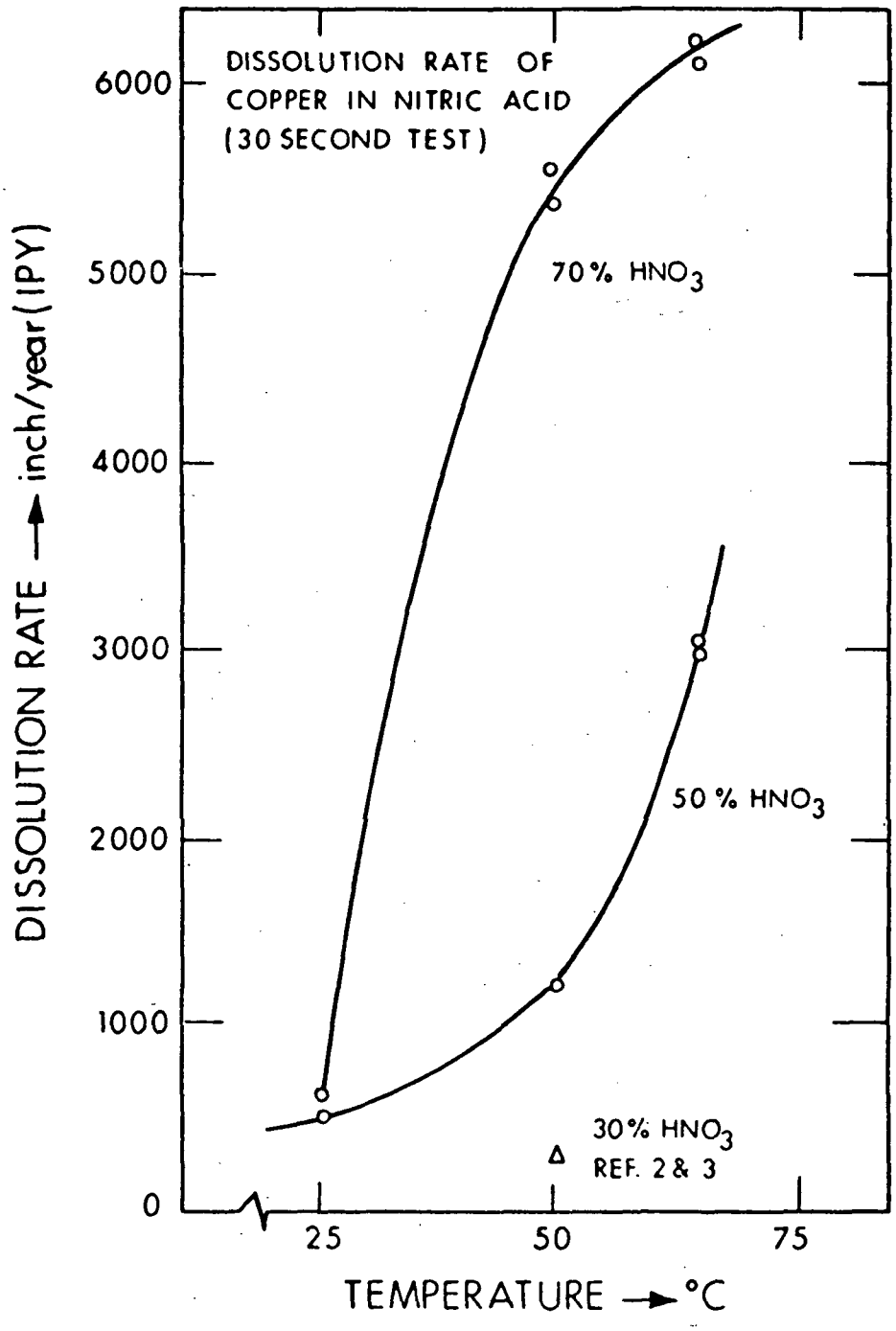

Figure 4. Dissolution Rate of Copper in Nitric Acid (30 Second Tests)

37184

concentration decreases. It is also apparent in Fig. 2 that the dissolution rate based on longer exposure times decreases, indicating that the aluminum forms a protective coating which progressively retards the dissolution rate.

The dissolution of copper is shown in Fig. 4. Note that the dissolution increases markedly with increasing temperature and that the dissolution rate for 70 percent is much greater than that for 50 percent. A corroborating comparable data point from the literature is difficult to find with most of the data reported being taken at much lower acid concentration levels (30 percent HNO_3 or less) (Refs. 2 and 3). The general trend at these lower concentration levels indicates increasing dissolution rates at increasing concentration levels.

3.1.2 DISSOLUTION OF ALUMINUM IN NITRIC ACID WITH VARYING CONCENTRATIONS OF COPPER NITRATE

The acid solution that the aluminum plated mandrel will be exposed to during the etching process will contain varying concentrations of copper nitrate ($Cu(NO_3)_2$). The copper nitrate molar concentration will increase from zero to about 0.2 during the complete dissolution of one copper mandrel. The question has arisen as to the possible deleterious effects of this constituent in the solution. To answer this question and to establish whether or not some means of removing the copper nitrate from the solution as it forms is necessary; the following series of tests were performed.

The dissolution rate of aluminum was measured in 50 percent and 70 percent HNO_3 at 25° and 50°C for $Cu(NO_3)_2$ molar concentrations up to 0.2. The results are shown in Figs. 5 and 6. As shown, the effect of increasing $Cu(NO_3)_2$ concentration is not pronounced. However, the effect of $Cu(NO_3)_2$ seems to be more detrimental to the aluminum at the lower acid concentration level.

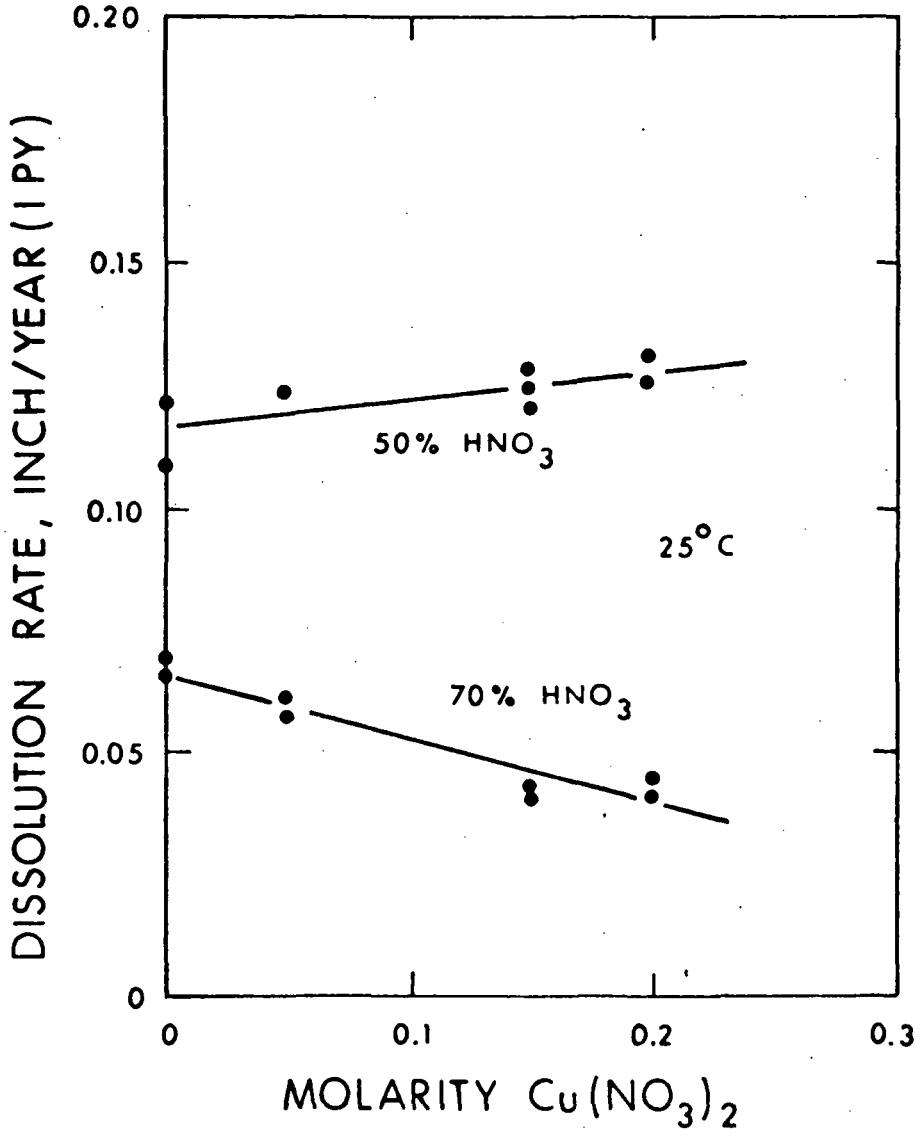

Figure 5. Effect of Copper Nitrate on Dissolution Rate of Aluminum

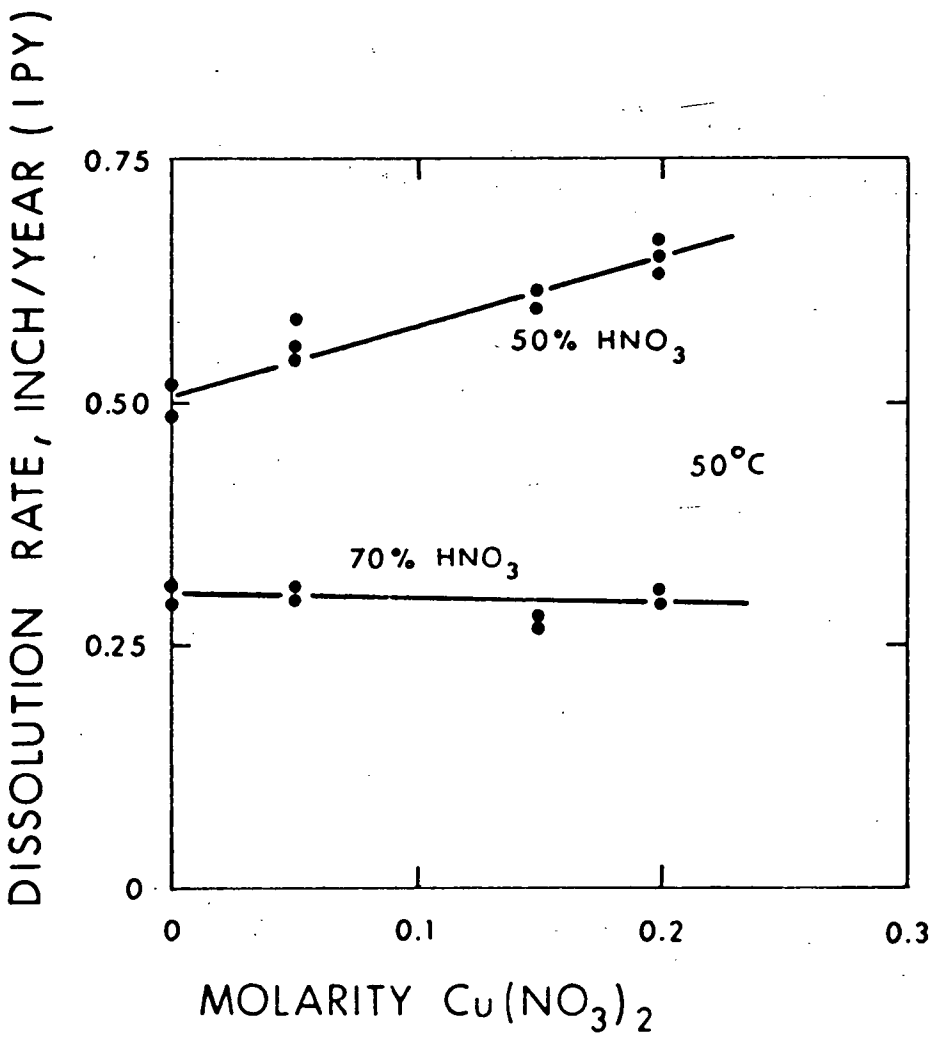

Figure 6. Effect of Copper Nitrate on Dissolution Rate of Aluminum

3.1.3 DISSOLUTION RATES OF COPPER AND ALUMINUM IN CONTACT IN NITRIC ACID

In the aluminum plated copper mandrel configuration, the two metals in mutual contact in the acid solution form a battery. This battery effect was evaluated by physically creating a copper-aluminum-copper sandwich, as shown in the photograph, Fig. 7. The sandwich was created by clamping a 0.050 inch copper plate between two aluminum plates with aluminum screws. The edges were masked off with RTV silicone rubber to expose only the one side shown in the picture. It was established earlier that the reaction rate of copper is very much greater than that of aluminum. For instance, dissolution rates for copper were obtained from a 30 second exposure while most of the aluminum data is based on a 6 hour exposure time. By limiting the amount of exposed copper relative to the exposed aluminum, it was possible to run the test for sufficient time to obtain measurable results on the aluminum without completely dissolving the copper.

Dissolution rates for copper and aluminum in the sandwich form are shown in Figs. 8 and 9. Note that the rates for aluminum are higher by a factor of 2 or more over the rate for the singularly tested metal. A certain portion of this increase is to be expected due to the shorter exposure time (refer to Fig. 2). The data has been extrapolated to an equivalent 6 hour exposure time, and an actual increase of about 50 percent is estimated to be attributable to the battery effect. It is apparent that the dissolution rate of copper is unaffected by the battery effect. One of the more significant findings became apparent during this phase of the testing, to wit: under certain conditions a black oxide-like coating would form over the copper, completely stopping the copper dissolution. This coating could be rinsed off quite readily with distilled water; however, the coating would reform with the same effect under the same acid exposure conditions. This phenomenon has been observed on prior lightweight structure programs. In fact, in the past, the etching process included periodic rinsing of the aluminum-plated copper mandrel with water to reinitiate the dissolution process.

4707

Figure 7. Copper-Aluminum-Copper Sandwich with RTV Mask

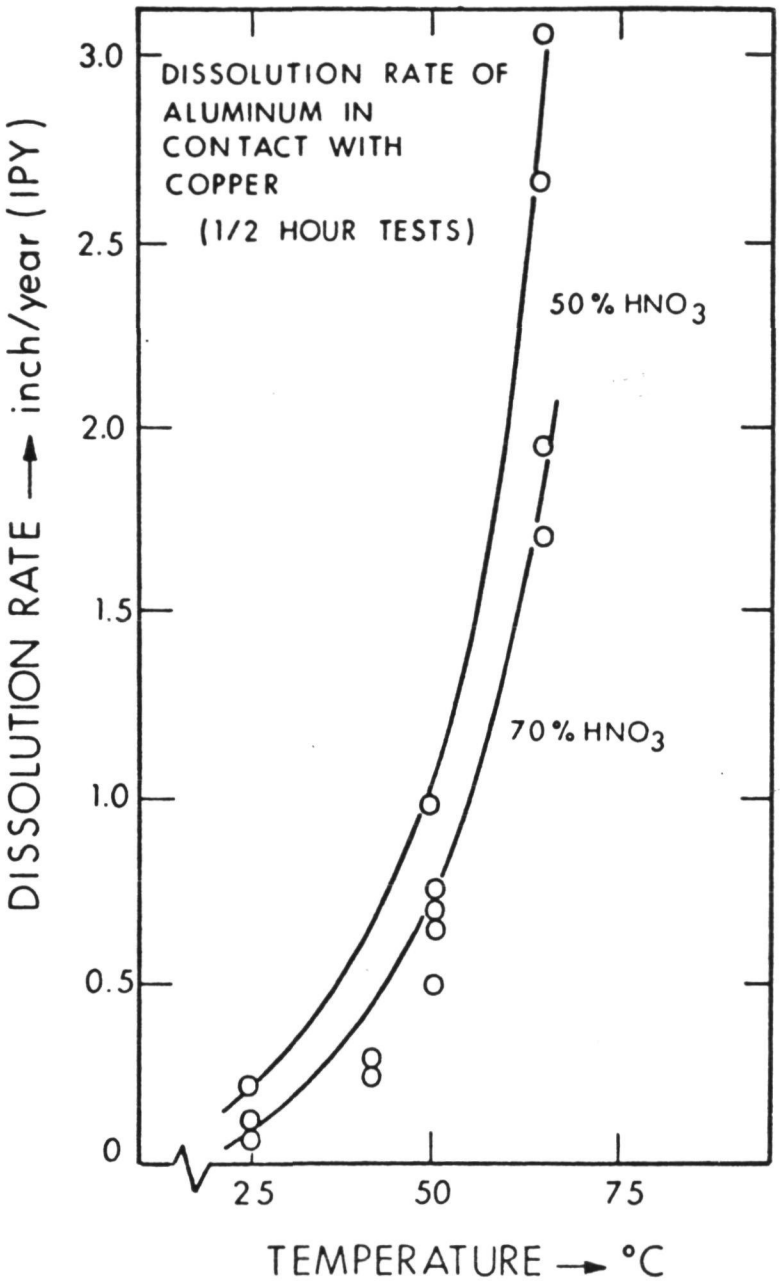

Figure 8. Dissolution Rate of Aluminum in Contact with Copper (1/2 Hour Tests)

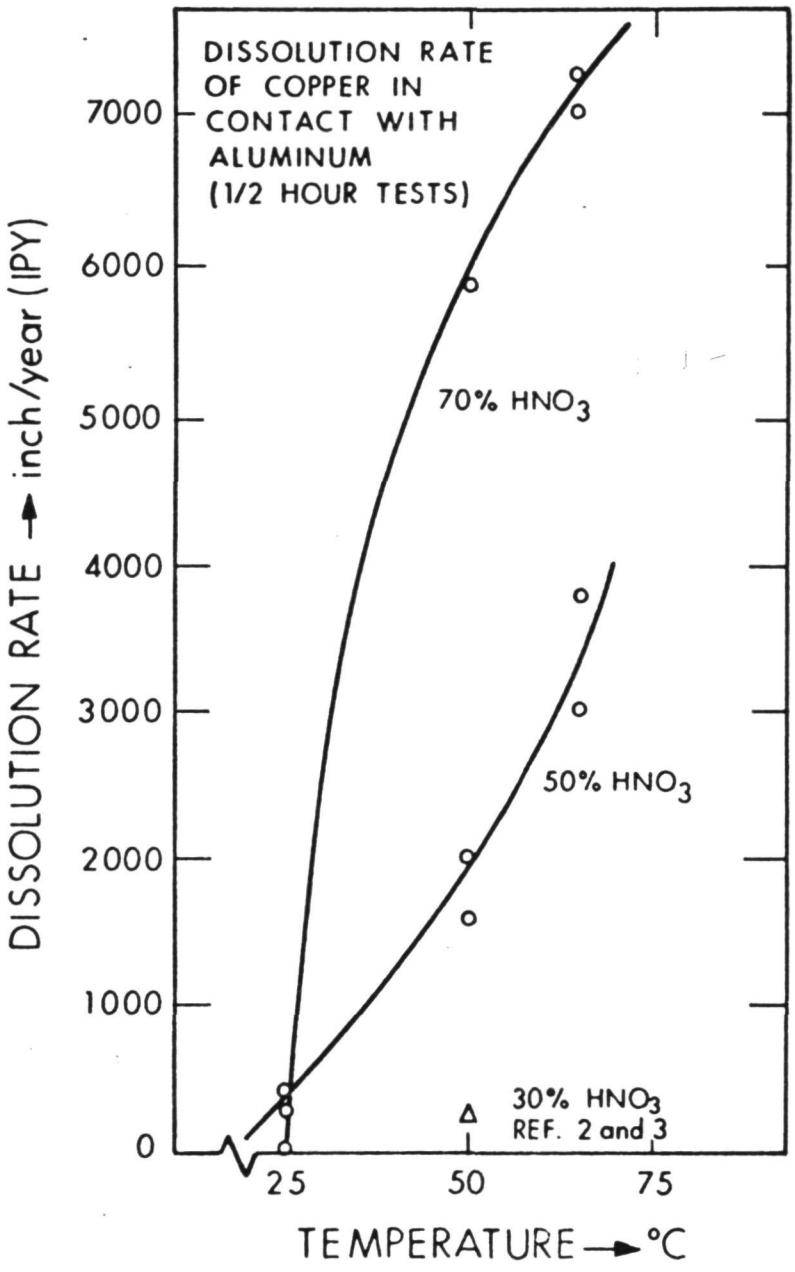

Figure 9. Dissolution Rate of Copper in Contact with Aluminum (1/2 Hour Tests)

During the test program just completed, the oxide-like coating was most likely to form at 70 percent HNO_3 and 25°C. The formation of this coating could be precluded by any one or more of the following:

a. Heating the acid bath to a temperature in excess of 40°C.
b. Reducing the acid concentration to 50 percent HNO_3.
c. Vigorously agitating the solution.

3.1.4 EXTENSION OF IDEALIZED LAB RESULTS TO HOLLOWCORE PANEL

Summarizing the results obtained from the first three steps, we find:

a. The HNO_3 acid attack on aluminum is lower with higher acidic concentration.
b. The dissolution rate of copper increases with increasing temperature and increasing acid concentration with the rate at 50°C and 70 percent nitric being appreciably higher than the rate for 50°C at 50 percent nitric.
c. A black oxide-like coating forms on the copper at the high acidic concentrations and lower temperatures. This coating can completely stop the copper dissolution.

   The coating formation can be precluded by elevating the acid temperature, lowering the acid concentration or vigorously agitating the solution.

Extending the observations noted above to the etching of an actual hollowcore panel, the following test conditions were selected:

Acid concentration:	70 percent HNO_3
Acid temperature:	50°C

The test specimen for this sequence of testing was taken from an aluminum electroplated copper hollowcore mandrel that was fabricated on a

prior contract. The first hollowcore panel etching was predicated on acid entering the aluminum hollowcore structure from the periphery. As long as 2 to 3 weeks were required to remove the copper under these conditions. Later, it was decided to drill a hole in each land space (as shown in Fig. 10a) to expose more copper to the acid and achieve the dissolution at a faster rate. With this "etching hole" drilled as shown, a symmetry is achieved which allows one to model the etching process for any size panel, as shown in Fig. 10b. A picture of the sample selected for testing is shown in Fig. 11. The edges were masked off with ethylene-propylene rubber to ensure that all etching would take place through the special hole drilled for this purpose.

The initial configuration tested had the hole drilled through one of the aluminum face sheets and halfway through the copper mandrel, as shown in Fig. 12a. Visual observation during testing of this configuration showed the etching reaction slowing to a stop under acid temperature and concentration conditions that were not anticipated, based on prior tests. Examination of the copper showed the black oxide-like coating previously discussed. The buildup of this coating is attributed to the gases formed by the reaction of copper with nitric acid.

Gases formed by the initial reaction completely fill the small cavity and stop the reaction which apparently gives the black coating a chance to start to form. The gas bubble escapes, liquid fills the cavity, and the process repeats. This continues until there is a sufficient build-up of the coating to completely stop the reaction. The final static condition is shown in Fig. 12b.

This condition was eliminated by drilling the special etching hole through both aluminum face sheets and completely through the copper mandrel, as shown in Fig. 12c. This configuration has a chimney-like effect, drawing liquid in the bottom and forcing the gases out the top. The reaction does not stop and is carried to completion. Figure 13

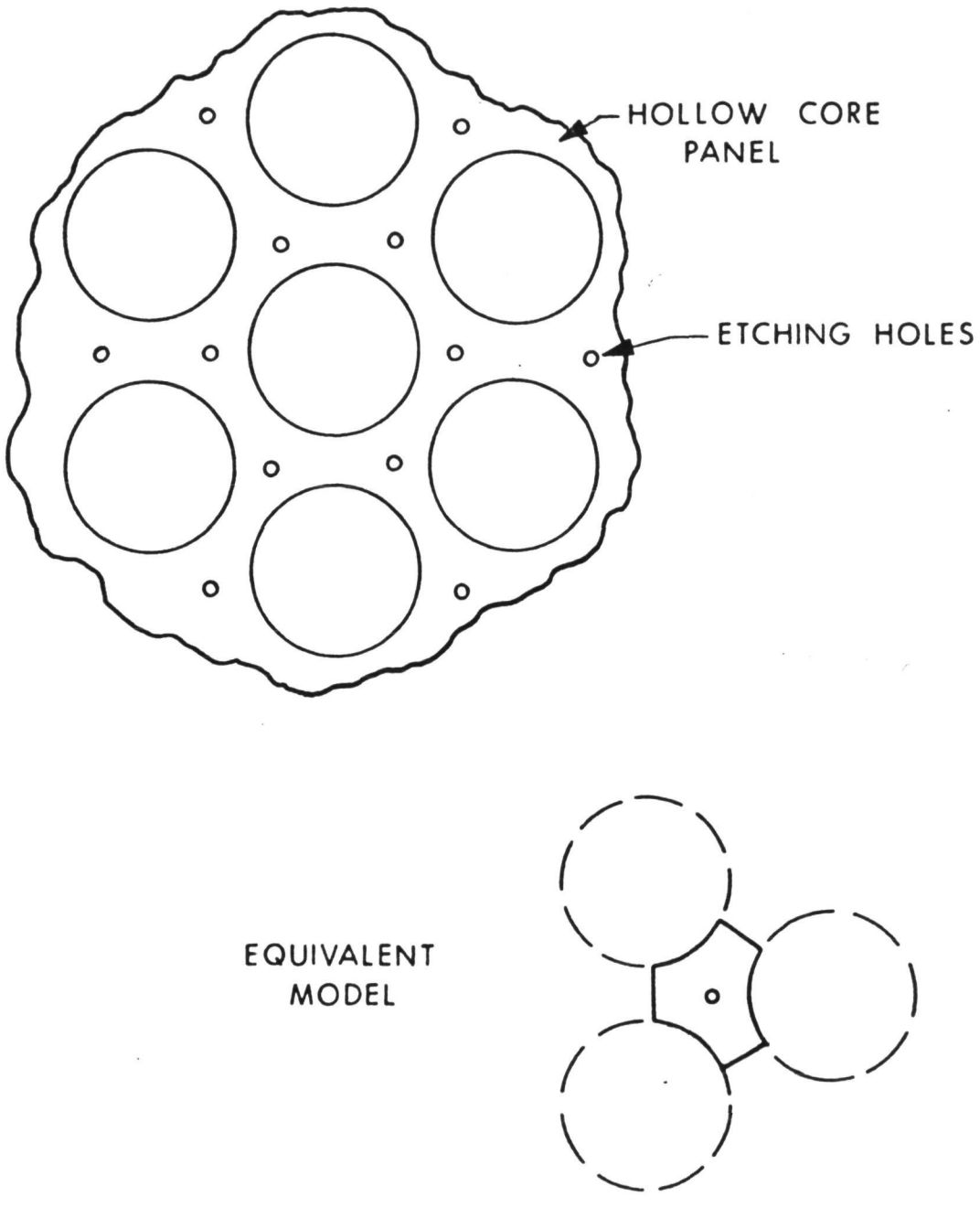

Figure 10. Electroplated Copper Hollowcore Mandrel with Drilled Land Spaces and the Symmetry Achieved

4706

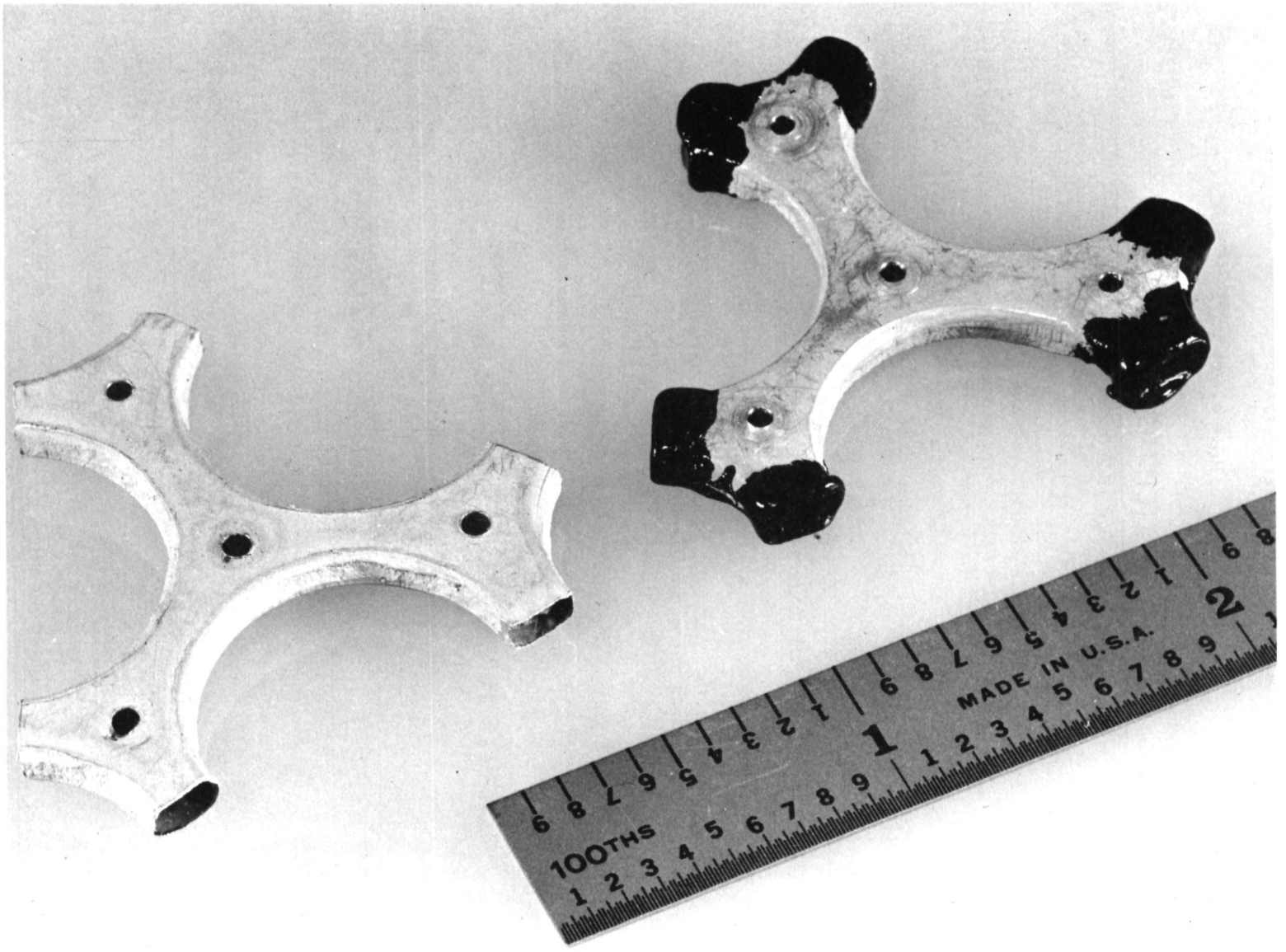

Figure 11. Samples of Hollowcore Panel, Masked with Ethylene-Propylene Rubber and Unmasked, Selected for Testing

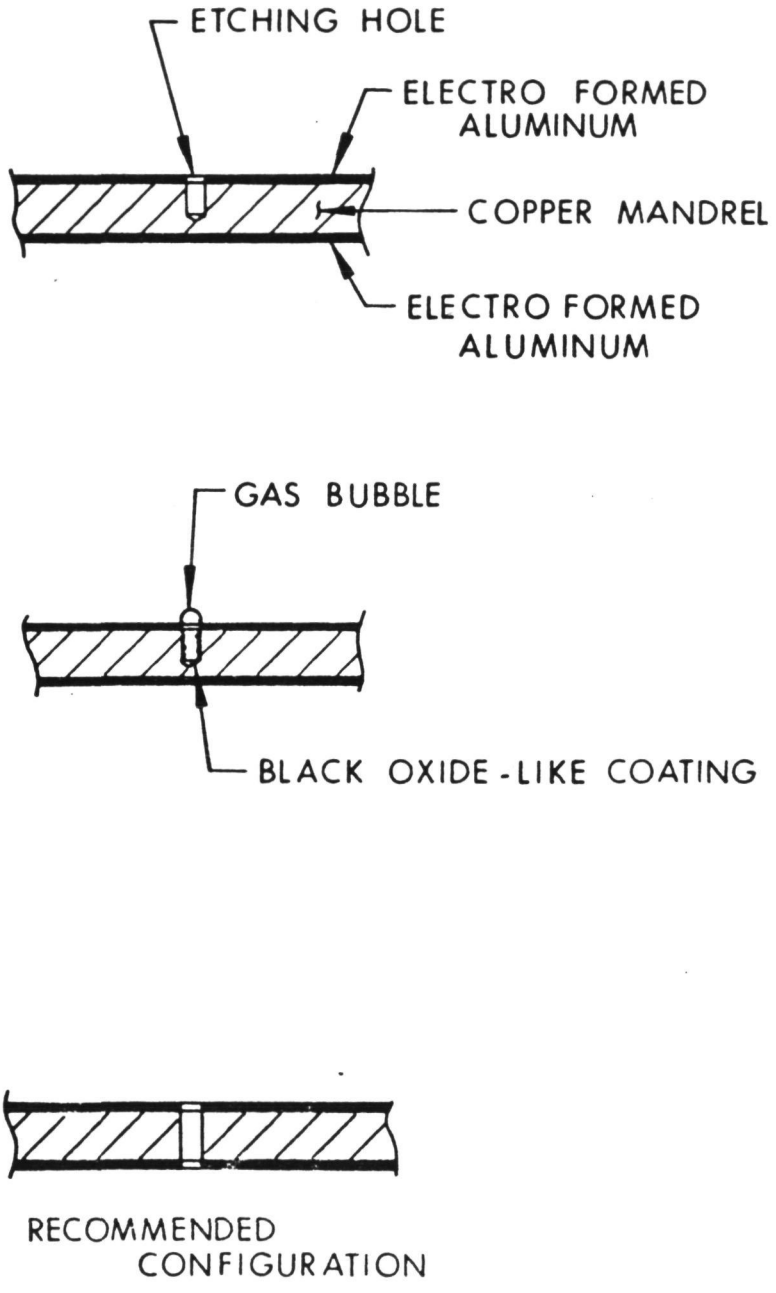

Figure 12. Geometry of Hollowcore Etching Holes

178

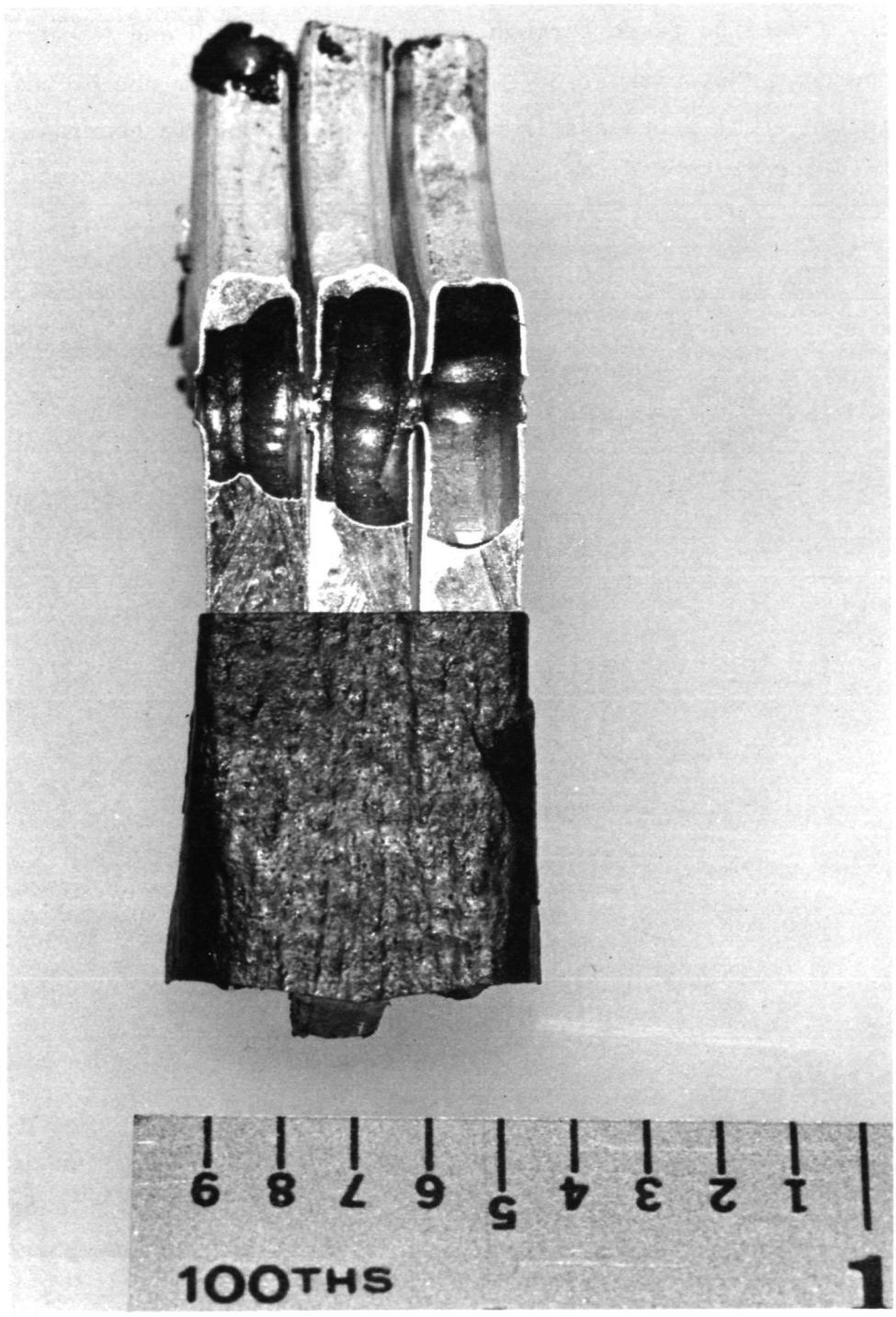

Figure 13. Three Hollowcore Etching Samples Showing Progress of Etching at 10, 20, and 40 Minutes

shows a section taken through 3 samples at 10, 20 and 40 minutes in a 70 percent HNO_3 bath at $50^{o}C$. It is apparent from the 40 minute sample that the etching process is nearly complete, and in general 1 hour is considered to be the nominal etching time for the copper mandrel.

A 6 by 9 inch sample was etched out in a flat pan to verify the scaling model. The resulting hollowcore sample is shown in Fig. 14. The copper mandrel was etched out in a little over 1 hour with the edge members completely sealed with ethylene-propylene rubber.

The recommended etch configuration, based on the result of the studies just described, is as follows:

a.	Acid concentration:	70 percent HNO_3
b.	Acid temperature:	$50^{o}C$
c.	Mandrel preheated	
d.	Aluminum plated copper mandrel configuration:	a through hole in each land area

For the conditions recommended, it is anticipated that virtually any size hollowcore panel may be etched completely free of copper in approximately 1 hour.

3.2 ALTERNATE MANDREL MATERIAL EVALUATION

Concurrent with the copper mandrel experimental evaluation described in the previous section, the literature was surveyed to identify potential alternate mandrel materials. This literature survey material evaluation included metals, plastics, and the respective etchant for each candidate mandrel material. The conclusion reached was that the copper-nitric acid system presently used is the most appropriate.

4705

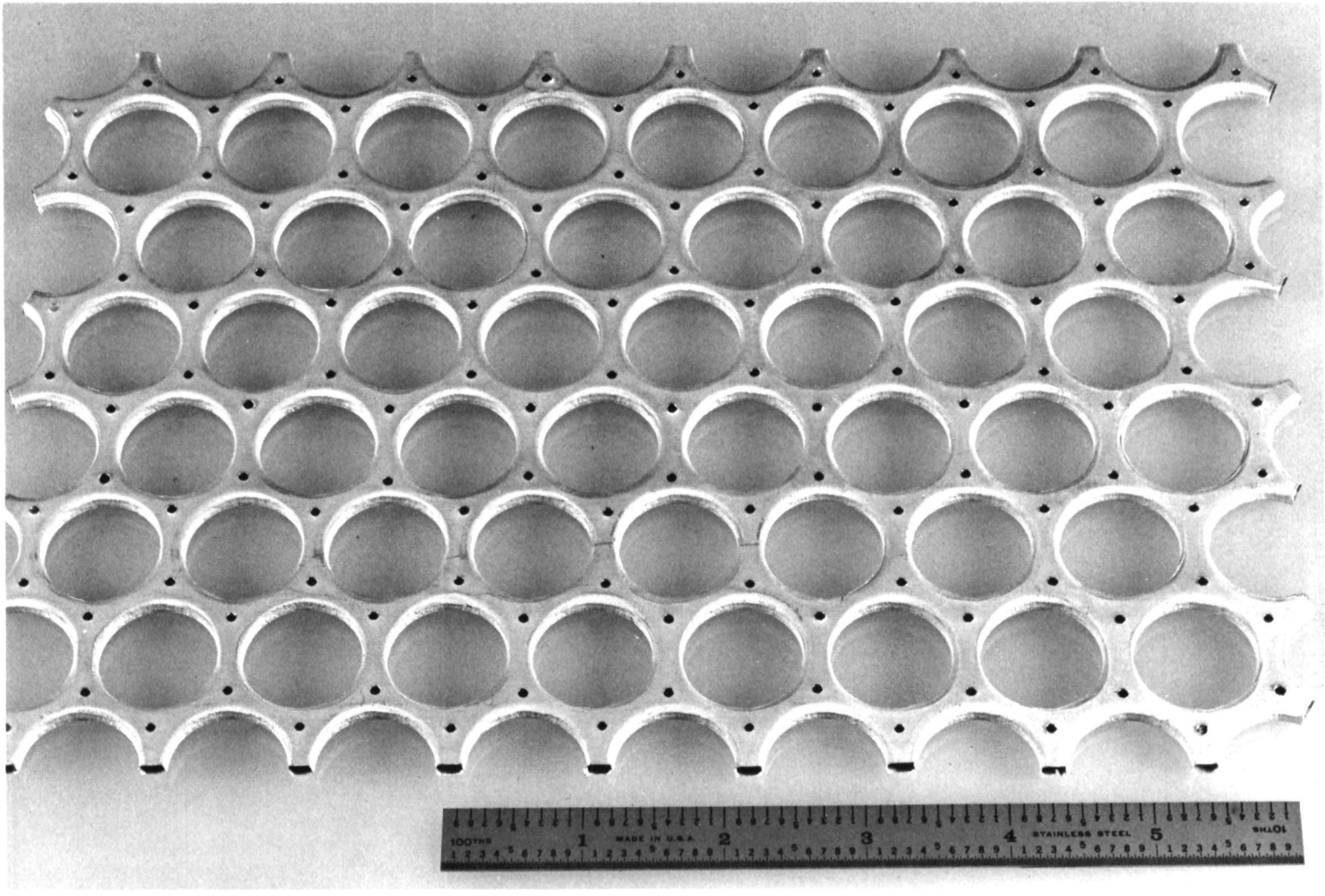

Figure 14. 6 inch by 8 inch Hollowcore Sample Etched in Approximately One Hour

Metal dissolution rate data for various etchants is summarized in Table I. Note that, of the group evaluated, the copper-nitric acid dissolution rate is the highest, leading to the general conclusion noted above.

The potential use of plastics as a mandrel material was also pursued. Styrene, acrylic, polypropyline, and ABS plastics were considered. Etching solutions for these materials include toluene, methyl-ethyl-ketone, acetone, and the chlorinated ketones. Dental wax and the "lost wax" material used in investment casting were also considered. The principal advantages to be gained from using plastic materials is the low material cost plus the fact that they could be made quite cheaply once the appropriate molding techniques were developed.

Principal disadvantages to the use of plastic materials include:

a. The general hollowcore configuration is difficult to cast or mold.

b. The resulting molded structure would be quite fragile and as such would present handling problems.

c. These materials require a conductive coating prior to aluminum deposition.

d. The ether plating solution would dissolve many candidate materials and the methods that may be developed for the prevention of same could deter the eventual etching process.

e. Initial tooling costs for injection molding or casting would be quite high ($10,000 is a representative cost for the 5 by 5 ft configuration being fabricated under this contract). Further, the tooling cost would not be recoverable if a different configuration were required.

These rather negative aspects, coupled with the positive result from the copper mandrel evaluation study, lead to the following conclusion:

TABLE I

ALTERNATE MANDREL MATERIAL
DISSOLUTION RATE SUMMARY

Material	Etchant	Temperature (°C)	Dissolution Rate (ipy)
Copper	30% HNO_3	25	116
Iron	38% H_2SO_4	60	25
Lead	27% HNO_3	25	14.3*
			54.5
Copper	4% NH_4OH	25	10.6
Magnesium	Salt Water		9.7
Iron	27% HNO_3		1.15
Aluminum	30% HNO_3	25	0.11
Aluminum	70% HNO_3	25	0.03
Aluminum	38% H_2SO_4	50	0.5

* with agitation

The optimization of the copper mandrel-nitric acid etchant system should be expanded to include an optimum mandrel fabrication configuration. This optimized fabrication configuration, coupled with the optimal etching procedure recommended in the previous section will lead to minimum panel fabrication time and minimum costs.

3.3 MANDREL OPTIMIZATION SUMMARY

An optimal structural hollowcore mandrel configuration has been established (Ref. 4). This particular configuration leads to a minimum weight panel, but has the disadvantage of being difficult and expensive to produce.

One of the more stringent fabrication requirements which must be met is the close tolerances associated with the hole center location and the hole maximum diameter, to wit: in the minimum weight configuration, the land width between holes is 0.050 inch. To prevent the overlapping or breakthrough that would accompany a relatively inexpensive machining process (such as punching) each hole is individually bored. This is time consuming and costly. In addition, the optimum structural configuration leads to a considerable dendritic growth at the edge of each hole diameter.

The time required to fabricate the copper mandrel can be decreased and the dendritic growth at the hole diameter can be eliminated by increasing the land width between holes. That is, if the land width is wider, the close tolerances on the hole locating dimensions and hole diameter can be relaxed. This would permit the use of more rapid, less expensive machining techniques. Better yet, there would be certain instances where "off the shelf" perforated sheet could be used. Using this approach, the techniques already developed for inducing the required mandrel curvature could be used. Standard perforated sheet stock has been used as mandrel material in the past. The wider land width

attendent with a mandrel of this type leads to better aluminum plating with virtually no dendritic growth at the hole diameters.

One step of the fabrication process would remain, however. The sharp corner at each hole diameter on each side of the mandrel must be radiused to prevent a stress concentration in the final aluminum hollowcore structure. It is anticipated that a relatively inexpensive hand tool can be developed for use by unskilled labor to achieve this result.

There is a weight penalty associated with the broader toleranced hollowcore panel. It has been established, however, by work done under prior contract and documented in Ref. 4 that optimal range on the minimum weight curve is rather broad. As a result, the incremental weight penalty on the final all up panel is not significant.

SECTION 4

PREPARATION OF HOLLOWCORE ETCHING EQUIPMENT

In the previous sections it was established that the copper mandrel can be etched out in a relatively short period of time. This is predicated on maintaining the acid at 50°C or greater. This conclusion was not anticipated and as a result certain previously conceived facility requirements have been eliminated and others have been altered. It was anticipated, based on past experience, that the etching process would require several days and that the acid bath temperature would have to be controlled over a rather narrow band. This would have required a complete heating and cooling unit with appropriate controls.

The results obtained eliminate the need for the cooling unit and simplify the heating requirements. The etching facility is shown schematically in Fig. 15. As shown, the facility consists of a tank, circulation pump, heater well for immersion heaters, thermostatic controls and acid supply drums. The tank is filled by the pump from the supply drums. The supply line enters the tank at the heater well, and the heaters control the acid temperature to a minimum of 50°C. Once the tank is filled the circulation pump maintains a constant circulation rate to preclude temperature and concentration gradients within the liquid in the tank. Photographs of the acid tank are shown in Figs. 16 and 17 with and without the hood.

A thorough investigation was conducted to ensure that the acid chilling unit was not required to prevent overheating of the acid. Some of the analytical efforts are herein summarized:

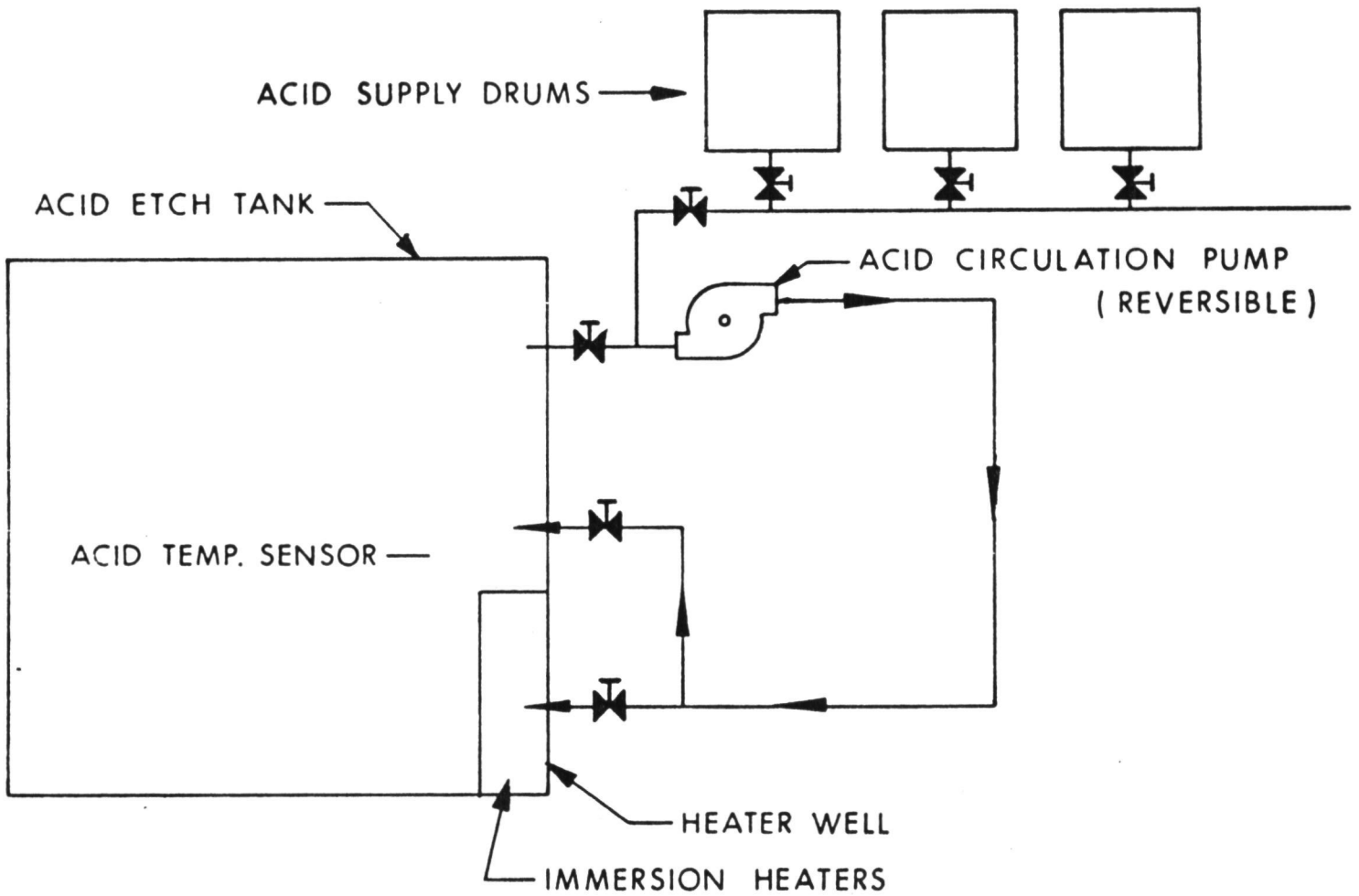

Figure 15. Acid Etch Facility Schematic

Figure 16. Etching Tank with Fume Hood Removed Showing Acid Heating Well

47015

Figure 17. Etching Tank with Fume Hood Installed

The chemical reaction describing the etching process:

$$4HNO_3 + Cu \rightarrow Cu(NO_3)_2 + N_2O_4 + 2H_2O + \text{heat}$$

The heat of reaction is:

1200 BTU/lb copper reacted

There are about 25 pounds of copper per 5 ft x 5 ft panel, hence:

30,000 BTU/hollowcore panel

It has been established in a previous section that about 1 hour will be required to completely dissolve a panel; hence, the average heat generation rate is approximately 30,000 BTU/hr. The acid tank, when filled, will hold about 3000 lb of nitric acid. If all of the heat generated by the dissolution of one copper mandrel were to be absorbed by 3000 lb of acid, the temperature rise of the acid would be about $9^{o}C$. With the initial acid temperature at $50^{o}C$, this $9^{o}C$ rise is completely acceptable. (Several hollowcore samples were etched at $85^{o}C$ with no deleterious effect.) In actual fact, however, the aluminum plated copper mandrel will be placed in the tank prior to filling. When the mandrel is in place the acid is added at a rate of about 10 gpm. At this fill rate it will take about 11 minutes to completely cover the mandrel with acid. The maximum acid temperature rise rate will occur during this first 11 minutes, and the largest part of the $9^{o}C$ temperature rise will occur during this time.

Page intentionally left blank

SECTION 5

DEVELOPMENT OF TECHNIQUES AND PROCEDURES FOR SOLUTION ANALYSIS

5.1 SOLUTION PREPARATION

In order to predict and control the material characteristics of the finished electroform, it is necessary to institute in-process check points in the solution preparation and plating procedures. The flow diagram for this process, from the receiving of raw materials through the plating of the work piece, is shown in Fig. 18. Typical values of mix ratios for preparing the hardened aluminum bath are shown on the flow diagram. Four quantitative evaluations of the aluminum plating solution, or of the raw materials which form the solution, or of the solution, are identified in this diagram. They are:

a. Peroxide content evaluation
b. Water content evaluation
c. Total aluminum content analysis
d. $LiAlH_4$ molarity

The procedures and equipment used for each of these quantitative analyses are given in the subsequent sections.

As shown in Fig. 18 the raw materials for the aluminum plating solution are inspected for damage and certification compliance. The chemicals are then transferred to a controlled storage area. Prior to beginning the mixing operation, the ether and anisole are checked for excessive peroxide and water content. An excessive amount of either peroxide or water is cause for rejection. Excessive peroxide in ether is a potential safety

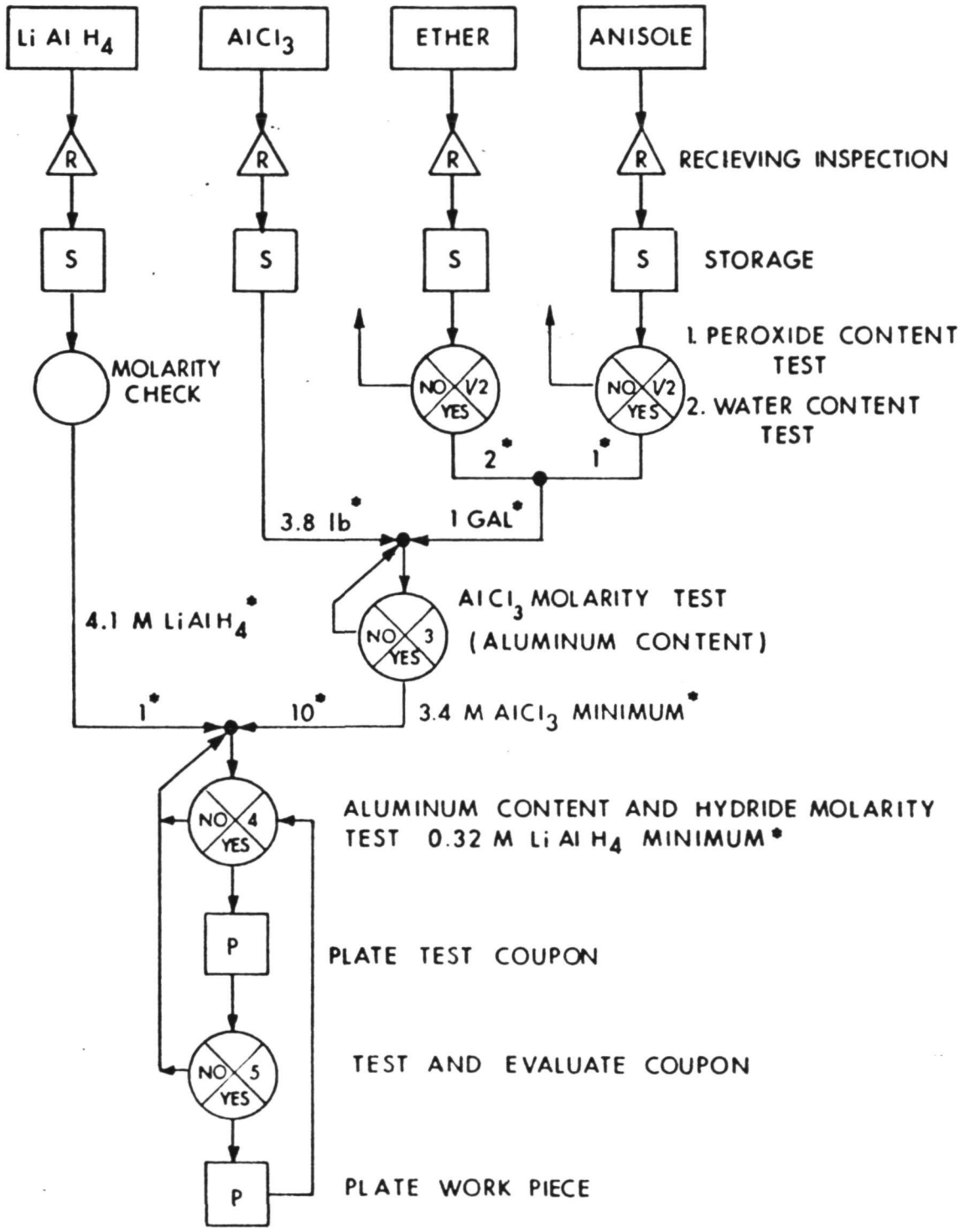

Figure 18. Aluminum Electroform Plating Solution - Makeup and In-Process Testing Flow Plan

38920

hazard. Excessive water in the ethers reacts with $LiAlH_4$ when added which necessitates the addition of excess hydride to achieve the desired concentration.

After the anhydrous diethyl ether and anisole are mixed in the ratio of two to one, anhydrous aluminum chloride powder is added in the amount of 3.8 pounds per gallon or greater. The resulting $AlCl_3$ molarity is deduced after determining total aluminum content. The $AlCl_3$ molarity should be at least 3.4M at this point, since further additions of $AlCl_3$ after the $LiAlH_4$ has been added have proved unsatisfactory.

The $LiAlH_4$ is purchased in ether solution at a concentration of 4.0M to 5.0M. A sampling of the hydride is analyzed prior to adding it to the solution to verify the molarity as certified by the manufacturer. The amount of $LiAlH_4$ solution to be added to the $AlCl_3$ is calculated to produce a minimum of 0.32M $LiAlH_4$ in the final solution. A check of total aluminum content and hydride molarity is made after the mix is complete. If the hydride molarity is not at least 0.32M, additional hydride is added.

After the solution is thoroughly mixed and filtered, a sample is drawn and returned to Pasadena where 2-inch by 6-inch flat plate samples are plated using the current density, bath temperature, and circulation rate which will be used for plating the final work piece. These samples are then tested to verify that the required strength and ductility have been achieved. If these properties do not meet specifications, further adjustments of hydride molarity and plating parameters can be made at this point. The work piece can now be plated in the large cell with reasonable assurance that an acceptable aluminum deposit will result. After each plating, a sample is taken and recycled through the molarity checks and test specimen check as shown in Fig. 18.

5.2 PEROXIDE ANALYSIS

Peroxide, if present in the ether or anisole solutions, can lead to explosions during subsequent operations. As a result, peroxide content above a certain level is sufficient to reject a batch of ether or anisole. The test procedure for peroxide analysis is as follows:

PROCEDURE

1. Transfer 10 ml of iron (II) thiocyanate to a glass-stoppered bottle from which the air has been displaced by carbon dioxide.
2. Fill the bottle to the brim with the solution (ether or anisole) to be investigated, and insert the stopper in such a way that no space remains above the liquid level.
3. Shake vigorously and allow it to stand for 5 minutes protected from the light.
4. If the ethereal phase is pink, the peroxide content is above 0.00015 percent. Peroxide content below this level is considered acceptable.

Preparation of Iron (II) Thiocyanate Reagent:

1. Mix 3 ml of 2.5M sulphuric acid with 35 ml of distilled water and boil to remove oxygen.
2. Dissolve 1 gram of iron (II) sulphate in the boiling solution and, after cooling, dissolve in it 0.5 gram potassium thiocyanate. The red color due to iron (III) thiocyanate is removed by adding small pieces of pure iron wire.
3. Store in an oxygen-free atmosphere.

5.3 WATER ANALYSIS

The purpose of this test is to determine the water content in either the diethyl ether or the anisole. The presence of water above a certain level in either of these fluids creates undesirable by-products when mixed with $AlCl_3$ or $LiAlH_4$. The method utilized is titration with a Karl Fischer reagent. This method is widely used for determining water content.

The basic Karl Fischer reagent is a solution of iodine, sulfur dioxide, and pryridine in methanol (in the Fisher Stabilized Reagent, Methyl Cellosolve). Iodine reacts with water in the presence of sulfur dioxide, while the pyridine combines with acid products which would reverse the reaction, and also serves as a carrier for the sulfur dioxide.

The dark brown to yellow iodine color of the reagent disappears as the iodine is reduced by water to colorless hydriodic acid. At the endpoint, when all the water has reacted, the dark color of free iodine persists. The titration is considered complete when the color remains for a predetermined length of time.

The laboratory test set up is shown in Figs. 19 and 20. As shown, the equipment consists of a reservoir, metering buret, stirring motor, and millivolt meter. The millivolt meter is used, rather than visual means, to indicate the change in potential that occurs when all of the water is reacted and free iodine exists in the fluid. The procedure for analyzing the water is as follows.

PROCEDURE

1. Fill reservoir with standarized Karl Fischer reagent.
2. Add 50 ml of the fluid to be analyzed to the reaction vessel.
3. Place glass and platinum electrodes in the fluid and connect to a millivolt meter.
4. While gently stirring the fluid, by means of the stirring motor and stirring bar, add the Karl Fischer solution at the rate of one drop every 10 seconds.
5. Continue adding the Karl Fischer solution until a marked change in millivolt output is noted on the meter.
6. Stop adding the Karl Fischer solution when the new millivolt output level is constant.
7. Convert number of drops of K.F. solution added to the water content of the solution being analyzed, i.e., one drop of K.F. solution reacts with X gm of H_2O in 50 ml of fluid. Therefore, the total number of grams of water in the 50 ml is equal to NX when N is the total number of drops added.

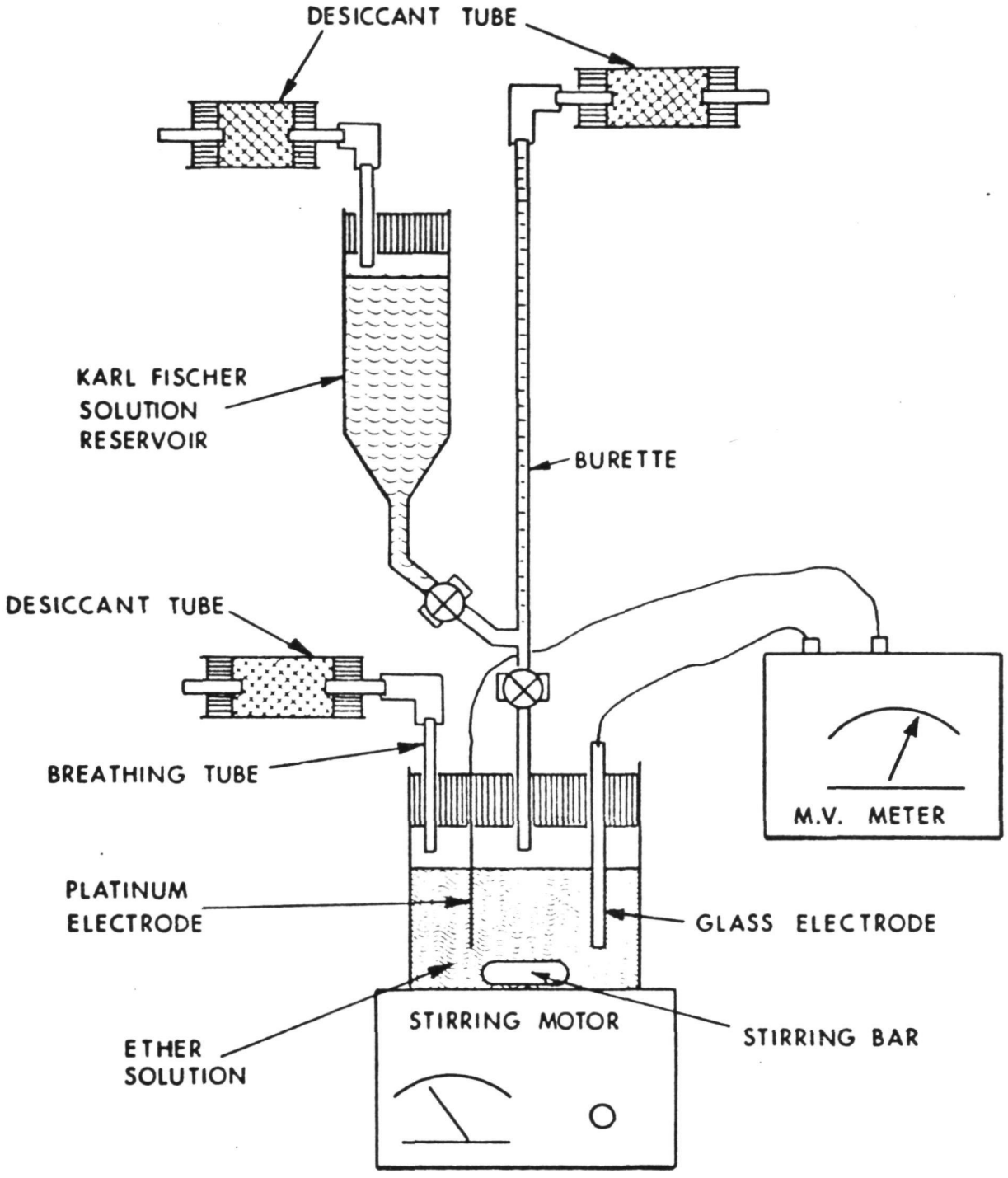

Figure 19. Block Diagram of Water Analysis Setup

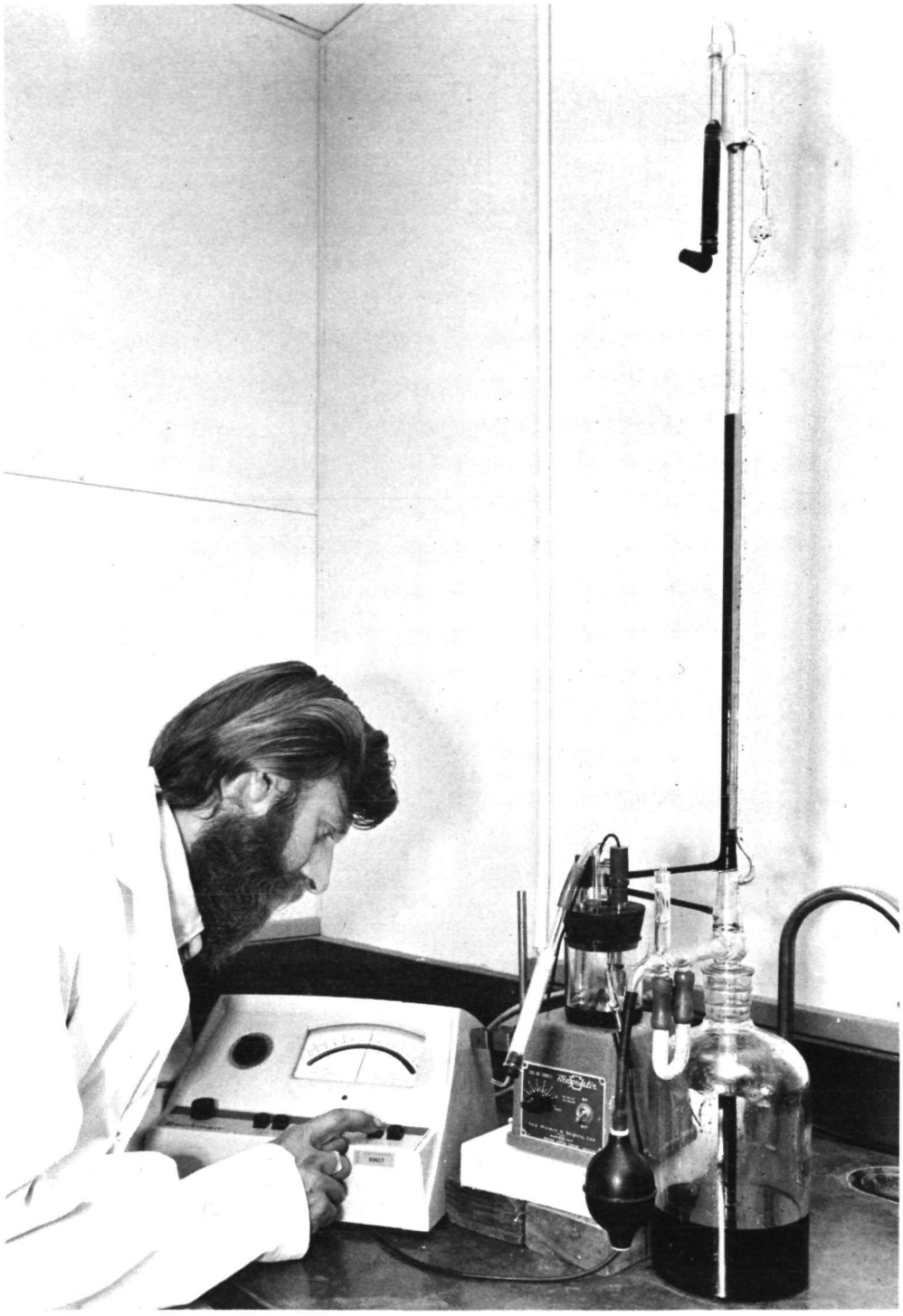

87013

Figure 20. Laboratory View of Water Analysis Setup

5.4 TOTAL ALUMINUM CONTENT ANALYSIS

The total aluminum content in either the aluminum chloride or lithium-aluminum hydride solution may be determined by a standard gravimetric analysis. (Standard colorimeteric or titrimetric analyses could also be used.) The gravimetric procedure is as follows.

PROCEDURE

1. To a 5 ml sample of either $AlCl_3$ or $LiAlH_4$, add H_2O drop wise until reaction stops.
2. After reaction is complete, dilute the solution to 50 ml.
3. Add 12.5 ml of solution containing 5 gm ammonium chloride per 200 ml H_2O.
4. Add 3 drops methyl red.
5. To the solution resulting from steps 1 to 4, carefully add diluted ammonium hydroxide drop until the solution has a whitish color. (The solution pH at this point will be between 6.5 and 7.5.)
6. Boil the solution for 1 to 2 minutes and filter at once on paper.
7. Wash the precipitate thoroughly with a hot 2 percent solution of ammonium chloride.
8. Wrap the moist precipitate in its paper, dry, char, and ignite, finally for 5 to 10 minutes at 1200°C.
9. Cool in a desiccator, weigh, and repeat the ignition until a constant weight is obtained.
10. The final residue is aluminum-oxide (Al_2O_3). The weight of aluminum in the residue can be deduced which can then be related to the total aluminum content in the solution being tested.

5.5 LITHIUM-ALUMINUM-HYDRIDE ANALYSIS

The lithium-aluminum-hydride ($LiAlH_4$) content is determined by reacting the plating solution with water. This reaction evolves hydrogen gas which is thoroughly dried and then reacted with copper-oxide which gives water vapor as a product of reaction. This water vapor is trapped in a desiccant tube and weighed. The water weight is then converted to $LiAlH_4$ molarity by stoichiometric analysis.

A photograph of the laboratory set-up is shown in Fig. 21 and a block diagram in Fig. 22. The procedure for analyzing $LiAlH_4$ is as follows.

PROCEDURE

1. The apparatus is set up as shown in figure 21. The weight of the second desiccant tube has been determined and recorded. The heating coil on the copper oxide tube has been energized and the CuO is glowing red.
2. Purge the system with helium gas. The test is ready to run when the weight change with time of the second desiccant tube reaches a minimum value. The helium gas runs continuously during the analysis.
3. Pipe the 15 ml of plating solution into reaction vessel and turn on the magnetic stirrer.
4. Add water drop wise through the pressurized separatory funnel until the reaction is complete. This will take about 10 minutes.
5. Continue the helium purge for at least 5 minutes after the reaction ceases.
6. The second desiccant tube is weighed and the gain is recorded as water.

The basic stoichiometric equations are as follows:

Water and lithium-aluminum-hydride

$$LiAlH_4 + 4H_2O \rightarrow LiOH + Al(OH)_3 + 4H_2$$

Copper oxide and hydrogen gas

$$CuO + H_2 \rightarrow Cu + H_2O$$

Hence, 1 mole of $LiAlH_4$ reacted will result in 4 moles of H_2O vapor evolved at the copper oxide tube.

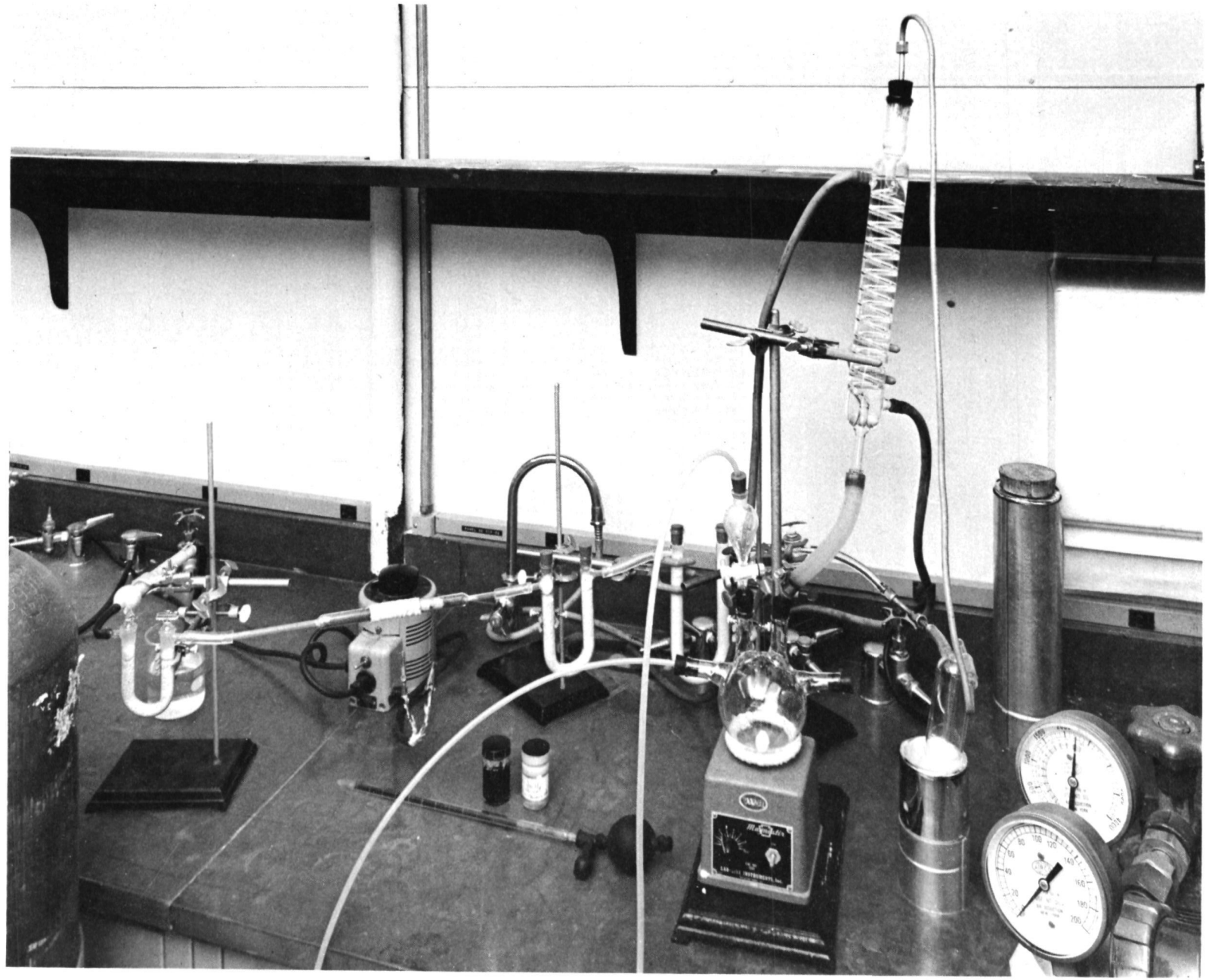

Figure 21. Laboratory View of Lithium-Sluminum-Hydride Analysis Setup

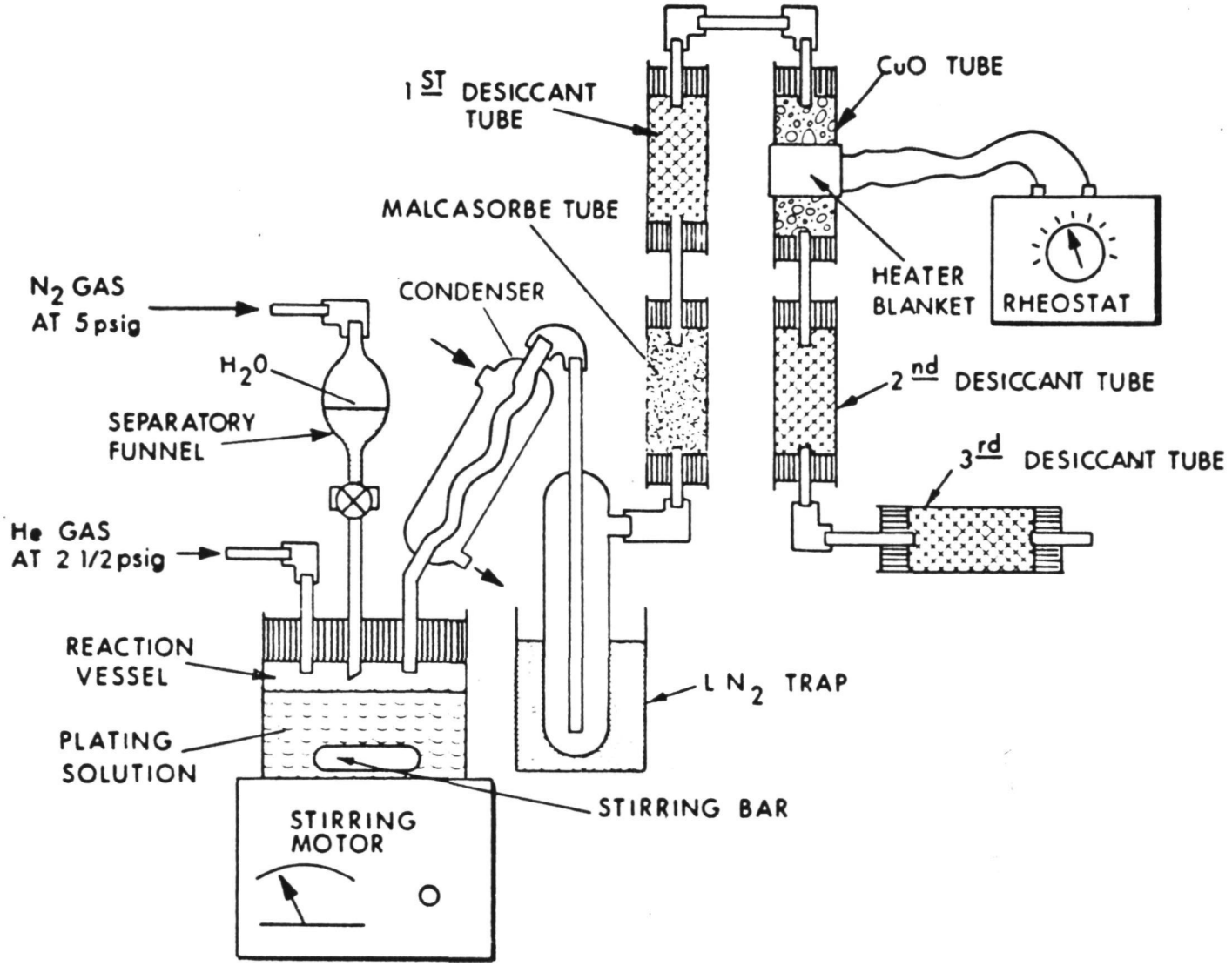

Figure 22. Block Diagram of Lithium-Aluminum-Hydride Analysis Setup

Page intentionally left blank

SECTION 6

EQUIPMENT MAINTENANCE AND MODIFICATION

6.1 MAINTENANCE AND MODIFICATIONS COMPLETED

At the start of this program it was determined that the 200-gallon mixing tank (reactor) was plugged at the base outlet and was completely filled with some form of the aluminum plating solution. A new top access flange was fabricated and installed that would permit removal of surface liquids out the top of the mixing tank. Approximately 150 gallons of liquid (mostly diethyl ether) was withdrawn.

After further inspection it was determined that approximately 50 gallons of solids and semi-solids were still in the mixing tank blocking any further outlet of liquid. The solids appeared to be mostly aluminum chloride hydrate slurry which had settled out of solution. A long-term leakage of moisture through the seal around the agitation drive is believed to have caused the formation of hydrate.

The normal outlet pipe at the bottom of the mixing tank was disconnected from the rest of the plumbing system and a combination water inlet and liquid release manifold was attached at the base outlet. Using a carefully controlled technique of combining nitrogen gas pressure at the top of the trapped solids and pressurized water injection at the base of the solids the blockage was slowly dissolved. Violent exothermic chemical reactions occurred each time water was permitted to come into contact with the aluminum chloride. Monitoring the tank outlet temperature-pressure readings and careful regulation of the water inlet was required during this process in order to avoid damage to the mixing tank. After the blockage was removed from

the outlet, the unit was opened and cleaned first with water and later with acetone. All flange gaskets were replaced and the stirring shaft gland was cleaned and tightened. Five additional inlet-outlet tubes were installed on the top of the mixing tank for increased versatility and emergency options possibilities.

Associated with the mixing tank leakage problem was damage to brass pipe fittings and stainless steel tubing in the system. Excess water reacts with the $AlCl_3$ to give HCl which attacks the fittings and tubing. Over 30 brass tubing fittings have been replaced with stainless steel fittings or eliminated in the total system by welding selected lengths of stainless steel tubing. Over 10 feet of pipe was replaced because of tubing wall failure and an additional 20 feet of new tubing was installed into the plumbing system. Most of the new tubing was installed as part of a plating tank bypass and secondary flowmeter system. The single speed plating solution pumps can now accommodate any size of plating tank at any flow rate up to six gallons per minute.

At the start of this program it was observed that three out of four solution temperature sensors were inoperative. As the leaking tube fittings were being replaced, each temperature sensor was removed from the system and carefully inspected. It was discovered that the three inoperative temperature sensors had been partially dissolved by the plating solution. The mercury that normally fills each temperature sensor had drained out into the aluminum plating solution. All inoperative sensors were removed and sent to the manufacturer for repair. One of the three was found to be damaged beyond repair. The other two were refilled with mercury, resealed, and recalibrated. The corrective action taken in order to prevent a repeat of this problem was the purchase of three stainless steel sheaths. A sensor sheath will positively protect the temperature sensors from further chemical attack.

As reported in the second quarterly, a new glove box was purchased for the Pomona blockhouse facility. It is a double window, four glove device with special modifications to permit installation on top of the aluminum chloride continuous feed system. The glove box was internally coated with Keysite 100 phenolic plastic. Special liquid feedthrough tubing fittings were installed between the base of the glove box and a modified flange plate on top of the mixing tank. The tubing fittings permit easy addition of lithium aluminum hydride from the glove box to the reactor or easy withdrawal of plating solution samples from the mixing tank into the glove box. The glove box has a transfer chamber with nitrogen gas and vacuum capabilities. The entire unit has been installed and has been used to process 2000 pounds of aluminum chloride to date in the current program. This unit is shown in Fig. 23 mounted on the aluminum chloride dry feeder. It is a positive aid to the difficult problem of plating solution preparation. Figure 24 shows the 60 gallon capacity plating tank installed in the plating facility system.

6.2 RECOMMENDED FUTURE MODIFICATIONS

To achieve more consistent and less expensive results with electroplated aluminum hollowcore structures, the plating cell in Pomona was evaluated and the following recommendations for modification are made.

a. At present, there is no way to prevent newly mixed aluminum plating solutions from being contaminated by the sludge and sediment built up in the underground storage tank from previous aluminum plating solutions. Therefore, to correct this problem, the following tasks must be accomplished.

   1. Open existing storage tank, clean and modify for better access (manhole, multiple inlets and outlets).
   2. Install an additional underground storage tank, with the same modifications as above, in order to accommodate different mixtures of aluminum plating solutions for different applications.
   3. Install an above-ground settling basin to trap any solids which pass through filters before they get into storage tanks.

Figure 23. Dual-Sided Glove Box Mounted on Solution Mixing Reactor

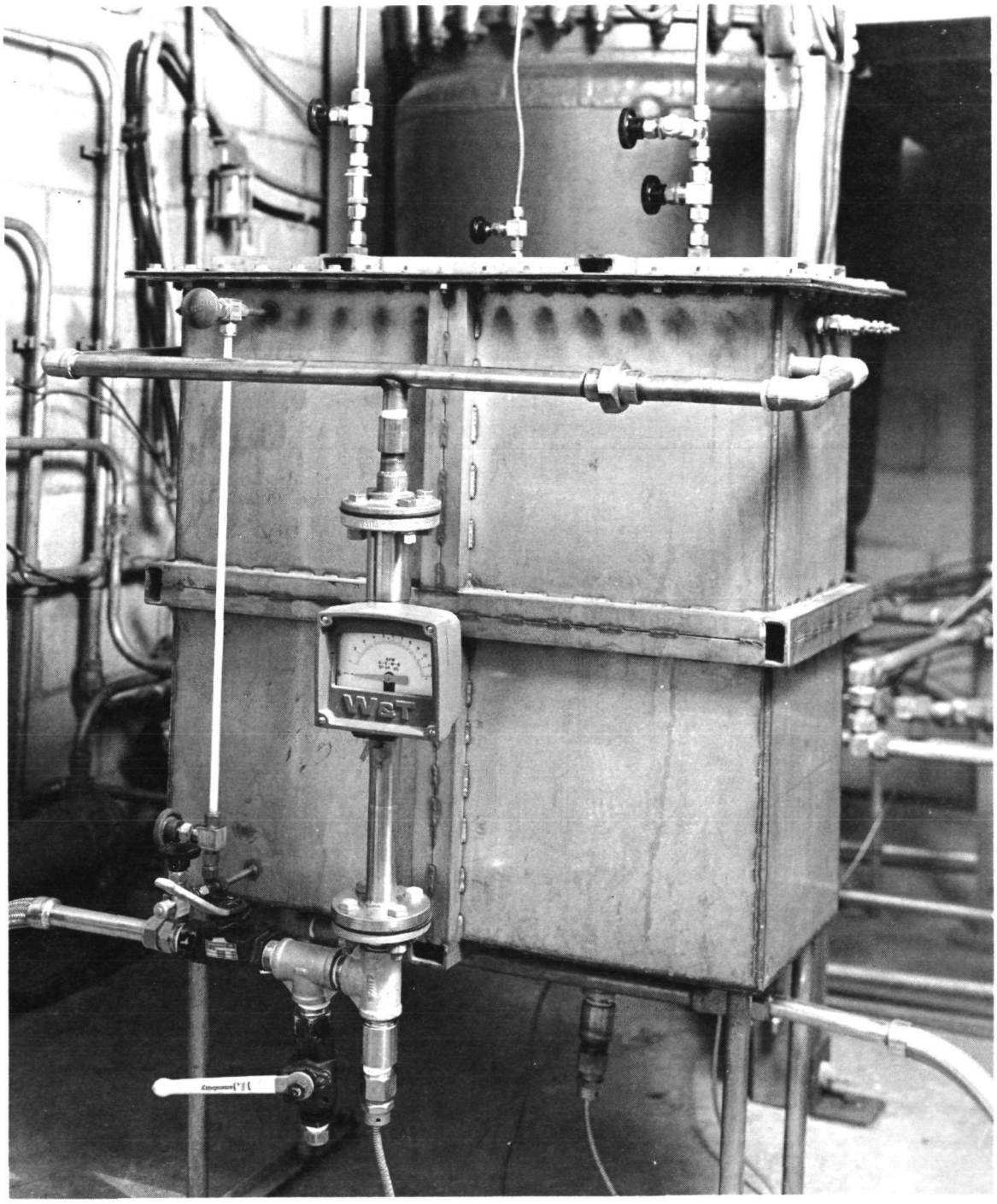

47013

Figure 24. 60 Gallon Capacity Plating Tank Installed in Blockhouse

4. Institute a regular maintenance schedule which would include agitation of the plating solutions within the storage tanks by the use of nitrogen gas and the circulation of solutions through clean filters.

b. Reassemble plumbing network utilizing the following improvements.

1. Install flange fittings on all major components such as filters, pumps and manifolds. This would eliminate the present brass fittings in the system which are being dissolved by the solution and would make periodic maintenance faster and more efficient.

2. Remount heat exchanger into a vertical position to permit complete drainage when the facility is closed down for short periods of time.

3. Replace 90^{o} angle elbows with welded radius bends to eliminate present solution restriction. The improved circulation would also help in maintaining constant solution temperature which is extremely important in producing a good aluminum plate.

c. Modify control panel with complete routing diagrams on face of panel for faster, safer, and more efficient operation.

d. Replace the fire hazard wooden platform inside the block house with welded metal supports and metal mesh flooring.

e. Obtain a second aluminum garage to serve as a clean room assembly area for all anode-cathode packages. The garage should also be modified (sink, electrical power, ventilation) so all nitric acid etching of aluminum plated copper mandrels could be accomplished in the same area.

f. Installation of a backup reserve vacuum system for safety and to insure against any failures during plating operations.

g. Install a hard mounted 300 ampere power supply cable with explosion-proof quick disconnect connectors. This would make electrical hookup of mandrel packages faster, more efficient, and definitely safer.

h. Install an open top waste pit for disposing of all waste plating solution.

i. Install a pedestal-mounted vise for the purpose of proper pipe assembly.

j. Purchase a helium leak detector so that entire system can be checked for leaks, thus preventing any atmospheric contamination of aluminum plating solution.

k. Install a cryogenic condenser in the present vacuum system just prior to the vacuum pump. This would stop all HCl fumes and ether gas (which presently cause the pump to break down periodically) from passing through pump.

l. Install a complete area intercommunication system, since at present it is impossible to communicate between areas during normal plating sequences or during periods of emergency conditions.

Page intentionally left blank

SECTION 7

PREPARATION OF 400 GALLONS OF ALUMINUM PLATING SOLUTION

During the term of this program, the preparation of 200-gallon mixing tank batches of plating solution was started four times using three different shipping lots of aluminum chloride. The first start was delayed before any chemicals were processed when the aluminum chloride was destroyed by water damage incurred when the Pomona Fire Department controlled a small fire in the chemical storage area. Identical aluminum chloride was reordered and a new storage area, separate from the hydride storage, was set up. The second start proceeded through the addition of $AlCl_3$ to the ether-aniosole mix. The process was stopped after the addition of 650 pounds of $AlCl_3$ when it was discovered that impurities and insolubles in the chloride were clogging parts of the plumbing system. In addition, further analysis indicated that one of the primary impurities was iron which reduced the hydride concentration by as much as 50 percent when $LiAlH_4$ was added. After clearing the plumbing of all slurry, the second start was pumped from the system and placed into storage carboys. No lithium aluminum hydride was added to the second mixing tank batch.

The plant manager of Stauffer Chemicals plant in Baton Rouge, Louisiana, was contacted to determine if a higher purity aluminum chloride powder could be obtained using their process without increasing the cost significantly. The answer to this question was that the chemical produced will vary in impurities with a corresponding variance in color, depending on the humidity at the time of processing. On high humidity days, iron rust from the handling equipment tends to be carried along with the powder. The commercial users of this material are not bothered

by these trace impurities. The best solution Stauffer could offer was to try to select the whiter material as processed and packaged for EOS use. An order for 2000 pounds of new chloride was placed with Stauffer on the basis that the whitest material available would be selected.

The third start, using a special third shipment of aluminum chloride selected for minimum iron impurity, was purchased from Stauffer Chemical Co. and processed into the mixing tank.

The following is a brief description of the third effort to prepare aluminum plating solution within the Pomona blockhouse facility. This solution was prepared using commercial grade anhydrous aluminum chloride from Stauffer Chemical Co. of Baton Rouse, Louisiana. The material had a yellowish color rather than the white-gray color specified. The ether-anisole portion of the plating solution was added to the mixing tank using normal procedures. The containers of aluminum chloride were selected and cleaned on the outside immediately prior to placement into the continuous feeder glove box. The 50-pound container was opened inside the glove box and the $AlCl_3$ powder fed into the mixing tank at a rate of just over 1 pound per minute. Four standard eight-hour work shifts were required to add all of the powder to the mixing tank. No problems were experienced during the continuous powder feed cycle. The addition of the last container of aluminum chloride was completed in the late afternoon of the fourth day. With the assumption that the powder would go into solution almost immediately, the total mix was allowed to stir for approximately two hours after the exothermic reaction had stopped, before being pumped out of the mixing tank and through the solution filter. This assumption proved to be very much in error.

In order to filter the solution, the routing was from the mixing tank, through the pump, filter, heat exchanger, main flow meter, high pressure solution distribution manifold and into the underground storage tank. As the solution was being pumped through the above detailed route, the undissolved chemicals, later estimated at approximately 50 pounds, accumulated at each bend and restriction throughout the entire route. Within 20 minutes, essentially the entire blockhouse plumbing system was plugged with a semi-solid paste. As more nitrogen gas pressure was applied to the source mixing tank, in an attempt to force the slurry through the plumbing system, more aluminum chloride would dissolve into the pressurized ether. The dissolving process is accompanied by an exothermic chemical reaction. The heat generated by this reaction within the plumbing system drove off the ether as a gas and resulted in a solid mass of cement-like aluminum chloride remaining in the plumbing system. The blocked portions of the plumbing system were disassembled and the blockage was easily removed with a water wash. The system was reassembled and the new solution was successfully pumped through the filters.

A six-liter sample of the partially prepared plating solution was taken to Pasadena for chemical analysis and sample plating solution preparation. The chemical analysis for the aluminum content of the Pomona plating solution indicated a molarity of 3.1M. This was approximately 20 percent lower than the calculated expected aluminum molarity. Following the aluminum analysis, lithium aluminum hydride was added to the 6 liter sample of the Pomona solution to a calculated level of 0.3M. A hydride analysis of the resultant solution indicated a molarity of only 50 percent of the calculated expected concentration. An additional equal amount of $LiAlH_4$ was added to the solution which brought the molarity up to 0.3M. The Pomona solution required double the normal amount of $LiAlH_4$ in order to bring the solution up to the

desired hydride concentration level. Plated samples were prepared and they were found to be acceptable. A sample aluminum plating solution mix was also prepared entirely in Pasadena from the Stauffer Chemical Company aluminum chloride. The calculated aluminum content should have been 4.5M. After analysis, the concentration was found to be 3.6M aluminum. The less than expected result was similar to that found in the Pomona solution. Next, lithium aluminum hydride was added to the plating solution mixture. After analysis, the hydride content was found to be approximately 50 percent lower than expected. A second equal amount of hydride was added to the Pasadena mix which brought it up to the required concentration. In both plating solution mixes, therefore, the aluminum content proved to be substantially lower than the calculated values and the amount of lithium aluminum hydride required in each mix was double the calculated values.

All of these solutions were blackish in color rather than the amber or brown color which is characteristic of this mix when using another manufacturer's high grade $AlCl_3$. A black fine sand-like insoluble could be filtered or allowed to settle out of solution but the black ink color remained.

Three 2 inch by 6 inch flat plate samples were electroformed out of the Pasadena mix. The tensile test results are shown in table II. These three samples (20, 21, and 22) were plated successively from the same bath with no additions. The first plating, sample 20, gave the highest ultimate strength of any of the samples tested in this program. The subsequent platings have slightly lower strengths and higher ductility, apparently due to the depletion of the iron impurity which increases the strength when codeposited with aluminum.

The solution prepared with this aluminum chloride would be completely acceptable for use in plating the 5 foot by 5 foot aluminum hollowcore. In fact, the high strengths achieved would be extremely desirable.

TABLE II

TENSILE STRENGTH TEST RESULTS

			Yield Strength		Tensile Strength		Elongation	
Sample Number	Actual Size	Actual Area	Actual Load Pounds	Pounds Per Sq In.	Actual Load Pounds	Pounds Per Sq In.	In__In 1	Percent
20	0.242 / 0.0040	0.000968	30.6	31600	33.0	34100	0.02	2.0
21	0.238 / 0.0042	0.00010	25.3	25300	28.3	28300	0.04	4.0
22	0.253 / 0.0048	0.00121	26.4	26400	28.9	28900	0.04	4.0

Yield Strength Determined by: 0.2% Offset

Tension Test At Room Temperature

However, the difficulties associated with the handling and filtering of the solution due to the insolubles and impurities and the fact that the impurities tend to react and deplete the hydride concentration, make the feasibility of continued use of this chloride questionable.

The possibility of using reagent grade anhydrous aluminum chloride was again investigated and rejected due to the high cost and lack of availability of large quantities of this material.

After the solution analysis was completed at the Pasadena facility, the program effort was continued in Pomona. The required amount of lithium aluminum hydride was added to the third batch of plating solution. The actual total amount of $LiAlH_4$ added was 50 percent more than the calculated quantity needed in order to have a molarity greater than 0.3M. This observation in Pomona agreed with the finding of the small quantity processed in Pasadena. After extensive stirring and filtering, it was observed in the filter cartridge that a precipitate of significant quantity was falling out of the completed mixture.

It was at this point that the major processing problems started in the Pomona facility. In the process of repeated filtering the new mixture, we were able to remove 15 to 20 gallons of a thick brown mud precipitate. The excessive filtering also required excessive solution pumping. The movement of 200 gallons or more of ether plating solution in either a closed circuit pumping mode (out the bottom of a tank, through the filter and into the top of the same tank) or from one container to another resulted in gradual evaporation of the di-ethyl ether portion of the aluminum plating solution. Two typical causes of solution evaporation during pumping cycles occur when moving solutions that may vary in viscosity (as when there is a heavy mud present). To move such solutions it is necessary to establish a pressure differential between source and receiving tanks. The lower pressure receiving tank

will tend to promote ether evaporation. Also, as the receiving tank is filling, it is necessary to constantly vent the pressure buildup as the tank fills with the liquid solution. The venting operation will also promote ether evaporation. Because neither the underground storage tank nor the mixing tank have a solution level indicator, the operator does not have any means of determining the extent of the solution loss due to evaporation. After most of the solids were filtered from the solution, a chemical and plating analysis was performed on the end result mixture. The plating solution was found to be usable. The small 60-gallon tank was set up in the plumbing system and an 18 inch by 22 inch hollowcore sample was plated out successfully.

The fourth attempt and last mixing tank batch was prepared with no trouble with the $AlCl_3$. The mixing and filtering methods used for this batch were completely changed so that it was processed with no difficulty. Seven hundred and fifty pounds of aluminum chloride was added to the reactor (mixing tank) for this batch. The attempt was made to have the stirring system run continuously overnight on the batch, however, the top seal on the stirring shaft would tend to overheat and leak gasses when it was left on. Therefore, the $AlCl_3$ addition cycle went as follows:

a. Add 200 pounds of powder and stir solution
b. Allow to sit overnight
c. Stir for approximately one-half hour in the morning
d. Filter the partially prepared solution
e. Add second 200 pounds of powder and stir
f. Allow to sit overnight
g. Stir for approximately one-half hour in the morning
h. Filter the partial solution
i. Add third 200 pounds of powder and stir

j. Allow to sit overnight
k. Stir for approximately one-half hour in the morning
l. Filter the partial solution
m. Add the last 150 pounds of powder to the mixing tank and stir
n. Allow to sit overnight
o. Stir for approximately one-half hour in the morning
p. Filter the partial solution
q. Take a sample of the solution for chemical evaluation

The aluminum chemical analysis proved the solution to be acceptable to that point. The calculated amount of lithium aluminum hydride was added to the partial mixture. Again, this calculated quantity proved to be inadequate. An additional equal amount of $LiAlH_4$ was added to the solution which brought the molarity up to 0.35M. The solution was then filtered and slowly combined with the previous mixing tank batch stored in the underground tank.

The next day the result of a delayed chemical reaction within the solution made itself evident by a thick brown mud precipitate beginning to show up in filled filter cartridges. The secondary reaction was so profuse that the underground storage tank outlet became solidly plugged. After a series of conventional attempts to unplug the underground outlet, the blockhouse plumbing system was modified in order to accept an outside source of high pressure nitrogen gas. By reverse pressurizing the underground tank outlet plumbing with 250 $lb/in.^2$ of nitrogen gas, the stoppage was forced back into the 600-gallon capacity underground storage tank. The total remaining quantity of prepared solution in the underground storage tank was then pumped and filtered for the next several days. The facility operators used a case of 60 filter cartridge elements in an attempt to get the heavy precipitate out of the prepared aluminum plating solution. Each filter cartridge holds six filter elements and approximately 3 gallons of packed solids when full.

As the solution was being cleaned up to a usable level, the new 400-gallon plating tank was being final assembled and pressure tested. The new tank was designed for heavy duty operation in both a pressure and vacuum mode. It had very rigid cold-rolled steel walls and top construction. The new tank was completely coated with Keysite 100 phenolic resin inside and out for complete chemical protection.

Immediately after the aluminum plating solution was prepared, the program effort was switched to Pasadena for the fabrication of the aluminum anodes and copper mandrel. The aluminum anode was formed and completely enclosed within teflon anode plating bags. The 5-foot by 5-foot copper mandrel had been previously machined with 2465 holes of 1-1/4 inch diameter. The mandrel was vacuum formed into the biconvex configuration and then each perforation and supporting webbing was very carefully hand cleaned mechanically and chemically. The completed anode-cathode package was wrapped in a plastic cover and transported to the Pomona facility. The three-piece anode-cathode package was bolted together with teflon fasteners and lowered into the new plating tank. The tank top was bolted down. The nitrogen gas, vacuum, plating solution inlets and outlet tubing and electrical power cables were attached to the tank. The entire plating tank system was again pressure tested. Everything at the plating facility appeared ready to go for the first plating effort in the large plating tank.

The solution was pumped from the underground storage tank through the filters and into the plating tank. All of the various plating tanks have solution level sight-glasses. This was the first time the new 400-gallon capacity tank had been connected into the plumbing system and also the first time the total available solution had been placed into a single container that had a solution level indicator. To the alarm of everyone involved, the total amount of solution available turned out to be not enough to cover the anode-cathode package inside

the tank. Apparently all the solution pumping, filtering, and heavy precipitate removal had caused excessive solution evaporation. The missing amount of solution was calculated to be about 150 gallons.

In an attempt to restore the minimum required aluminum plating solution volume, 50 gallons of additional di-ethyl ether and 100 gallons of partially prepared solution from the second mixing batch were carefully combined with the existing solution. After a short period of mixing the three new solution components together, 7 gallons of additional lithium aluminum hydride was slowly combined with the prepared solution. After further mixing and filtering, a solution sample was taken from the final mixture and returned to Pasadena for chemical and plating properties evaluation. After a thorough chemical analysis, it was determined that 12 gallons of additional $LiAlH_4$ was required in the prepared solution. The 7 gallons of hydride combined with the plating solution was the last quantity of $LiAlH_4$ available at EOS. If any further aluminum plating were to be done in the Pomona facility, it would be necessary to purchase an additional amount of 4.1M lithium aluminum hydride. At this point the program was stopped because of lack of funds for any further aluminum plating development effort. The plating facility has been closed and the 400 gallons of plating solution is in the underground storage tank.

SECTION 8

THERMAL TESTING; SURFACE PROPERTY MEASUREMENTS

8.1 ABSORPTIVITY AND EMISSIVITY

During this reporting period, radiation surface properties (absorptivity and emissivity) measurements were made on the component materials that are exposed on the rear or inactive side of a hollowcore solar panel. The materials tested were Kapton film backed up by actual and simulated solar cells and electrodeposited aluminum sheet. The electrodeposited aluminum sheet tested was in "as received" forms, smooth and dendritic, and both hard and soft anodized. The purpose of these tests was to establish surface properties for design calculations and to provide data for evaluating the relative merits of bare and anodized aluminum hollowcore panels.

A complete list of samples tested is summarized in Table III. As shown, there were three each of the groups noted above. All samples were tested on a Quick Emittance Inspection Device (Ref. 1) to obtain an indication of the total data spread and to provide a basis for determining the most representative sample of each group of three.

The samples selected as being representative of the average of their group were then measured spectrally. The solar absorptivity was determined by measuring the spectral reflectance from 0.28 to 25 microns and integrating over the solar irradiance (Ref. 2) to obtain the solar absorptivity. The normal emittance was determined in a similar fashion. Spectral measurements were made and integrated over the 300^{o}K Planckian Radiator function.

TABLE III

SAMPLES TESTED

Component Materials	Sample No's	Solar* Absorptance	Near-Normal Emittance		Hemispherical** Emittance
			Quick Emittance Inspection Device	Integrated Spectral Measurements	
Bare Electroformed Aluminum	1.		0.08_7†		
	2.		0.07_4		
	3.	0.16_3	0.08_4	0.06_7	0.08_4
Sulfuric Acid Anodized Electroformed Aluminum	4.		0.82_8		
	5.	0.34_3	0.83_3	0.83_3	0.80_0
	6.		0.83_3		
Chromic Acid Anodized Electroformed Aluminum	7.		0.78_4		
	8.		0.74_5		
	9.	0.41_3	0.75_8	0.72_6	0.70_8
Bare Dendritic Electroformed Aluminum	10.		0.23 ±0.05††		
	11.	0.34_3	0.27_5 ±0.03	0.21_3	0.24_1
Kapton Backed with Simulated Solar Cells	12.		0.87_4		
	13.		0.86_5		
	14.	0.53_1	0.87_0	0.88_1	0.83_8
Kapton Backed with Solar Cells	15.		0.88_0		
	16.		0.88_0		
	17.		0.88_0		

*Samples were selected on basis of QED measurements as representative of their group for α_s and ϵ_{HC} measurements - see discussion.

**Calculated according to Fig. 2 of Ref. 3.

†Although the accuracy of the measuring instruments does not justify three significant figures, the third figure is retained depressed so as to indicate trends.

††Variations of emittance across the test specimen.

Photographs of the actual and simulated solar cells tested are shown in Figs. 25 and 26. As shown, the solar cells were simulated by a 0.75 inch diameter aluminum disc. The purpose for simulating the actual cell was to obtain a configuration that was compatible with the test equipment, to wit: the 3/4 inch disc. Actual cells were also mounted on Kapton to serve as an indication of the degree of simulation via the Quick Emittance Inspection Device.

Results of the measurements are also tabulated in Table III. In the last column of the table, values are given for Hemispherical Emittance. These values were obtained by multiplying the spectrally determined near-normal emittance by the theoretically derived ratio shown in Fig. 2 of Ref. 3. Of particular interest in Table III is the degree to which the properties of the simulated solar cell configuration matched those of the actual configuration.

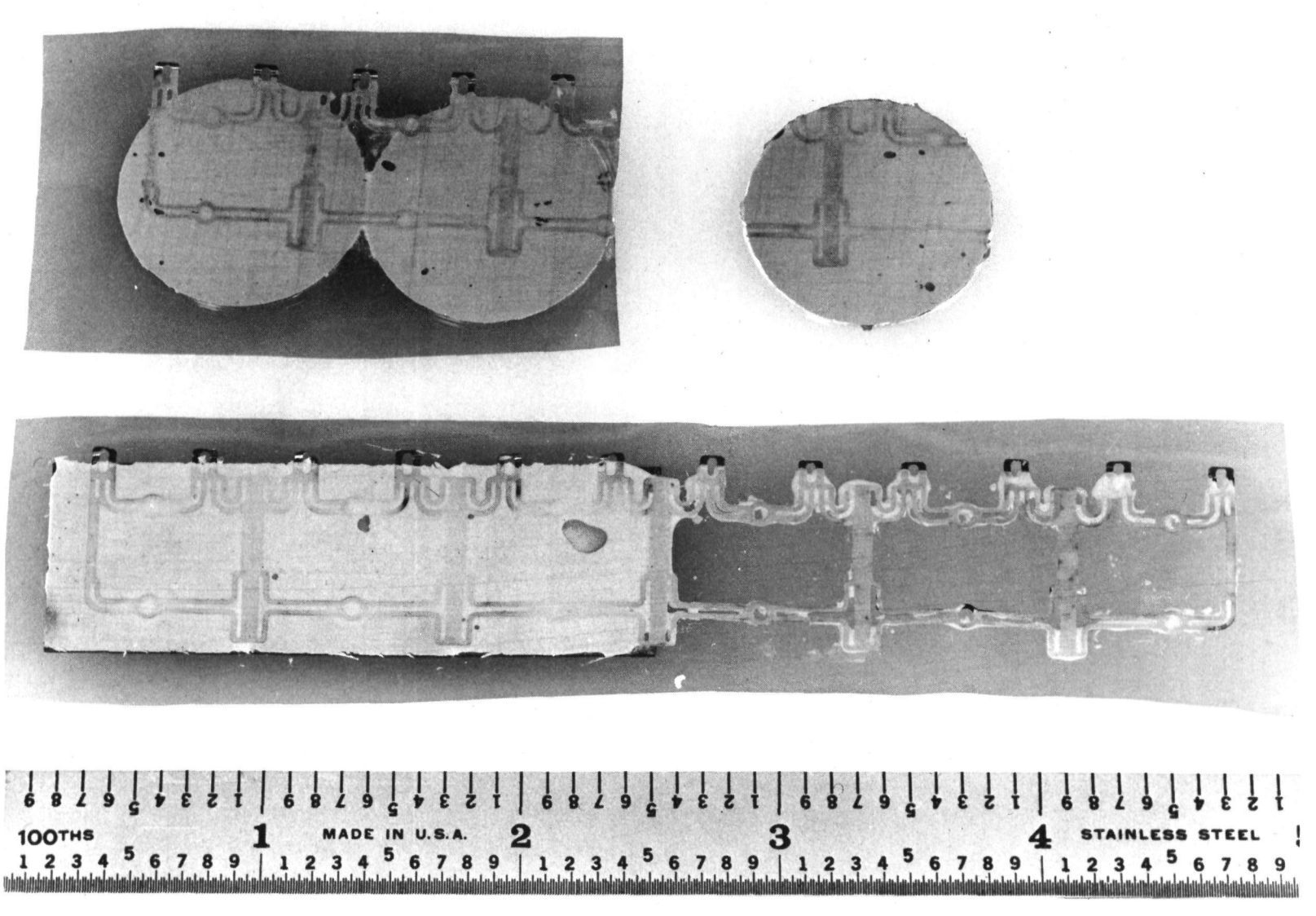

Figure 25. Actual Cells and Simulated Cells (back side)

6074

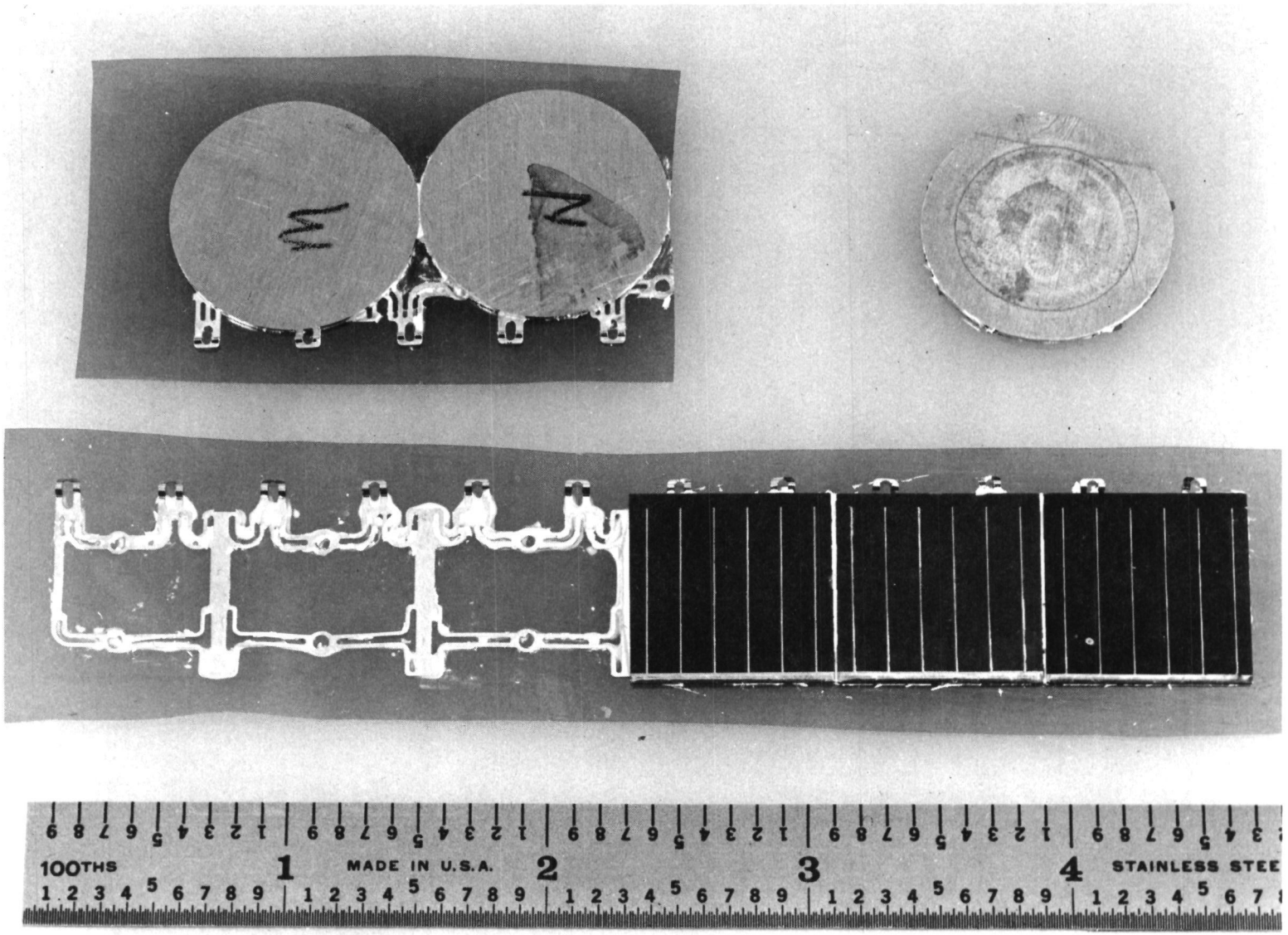

Figure 26. Actual Cells and Simulated Cells (front side)

Page intentionally left blank

SECTION 9

BASELINE CONFIGURATION FOR THREE-PANEL DEPLOYABLE ARRAY

The baseline configuration for the three-section deployable array is shown in EOS Drawing Nos. 4045-100, fully deployed; 4045-101, stowed; and 4045-102, partially deployed (Figs. 27 through 29).

The half-panel frame shown in the figures is an extension arm which serves the following purposes:

a. Deploying the active panels away from the body of the spacecraft to minimize shadowing.

b. Deploying the array from the center of the stowed volume in a manner which allows the center of gravity of each panel to move along a straight line away from the body of the spacecraft.

The deployment-retraction scheme shown in Figs. 28 and 29 use torsion springs at each hinge location to provide power for deployment. The deployment is controlled by the rates of payout of cables attached at each hinge line. When fully deployed, the cables form a guy-wire system which increases the stiffness of the deployed array. If retraction capability is desired, a single motor drive on the cable storage drum can be used to control the deployment rate and to provide power to rewind the cables and retract the array.

Tie downs for the launch configuration will be pyrotechnically released cables which are independent from the deployment-retraction cable system.


REVISIONS
ZONE
LTR
DESCRIPTION
DATE
APPROVED
NOTES: UNLESS OTHERWISE SPECIFIED
CELLS MOUNTED ON CONCAVE SURFACE
TOP VIEW OF ARRAY FULLY DEPLOYED
RETRACTION CABLE SYSTEM NOT SHOWN
CELLS MOUNTED ON CONVEX SURFACE
CELLS MOUNTED ON CONVEX SURFACE
2" DIA CURVED BERYLLIUM TUBING
TYPICAL OUTER FRAME FOR THREE ACTIVE PANELS.
2" DIA. STRAIGHT ALUMINUM TUBING.
TENSION CABLES.
TORSION SPRINGS FOR ARRAY DEPLOYMENT.
TWO PER HINGE JOINT.
MAGNESIUM HINGE FITTINGS - TYPICAL -
MATE WITH BERYLLIUM TUBING TO FORM PANEL CORNERS.
HINGE FITTING AVAILABLE FOR
ATTACHMENT OF ADDITIONAL ACTIVE PANELS.
SOLAR CELL MOUNTING AREA...
CELLS CAN BE MOUNTED ON EITHER
CONVEX OR CONCAVE SURFACE OF PANELS.
DIELECTRIC MATERIAL - TYPICAL.
ALUMINUM HOLLOWCORE SUBSTRATE - TYPICAL.
ALUMINUM MOLDING - TYPICAL
MATES HOLLOWCORE SUBSTRATE WITH BERYLLIUM TUBING.
HALF PANEL FRAME
FOR DEPLOYMENT SYSTEM ONLY -
NO SUBSTRATE OR SOLAR CELLS
FIRST ACTIVE PANEL
CELLS MOUNTED ON CONVEX SURFACE
SECOND ACTIVE PANEL
CELLS MOUNTED ON CONCAVE SURFACE
THIRD ACTIVE PANEL
CELLS MOUNTED ON CONVEX SURFACE
FRONT VIEW OF ARRAY FULLY DEPLOYED
RETRACTION CABLE SYSTEM NOT SHOWN
4045-100
QTY REQD
SYM
CODE IDENT
PART OR IDENTIFYING NO.
NOMENCLATURE OR DESCRIPTION
MATERIAL
SPECIFICATION
UNIT WT
ZONE
ITEM NO.
LIST OF MATERIALS
UNLESS OTHERWISE NOTED
LINEAR DIMS. IN INCHES
TOLERANCES
DECIMAL
FINISH
ANGULAR
DO NOT SCALE
MATERIAL
TREATMENT, FINISH
SIMILAR TO
ACT. WT
CALC. WT.
CONTRACT NO.
DRAWN
DATE
CHECK
DESIGN
DESIGN ACTIVITY APPD
CUSTOMER
ELECTRO-OPTICAL SYSTEMS, INC.
A XEROX COMPANY
TITLE
LIGHTWEIGHT ALUMINUM
HOLLOWCORE SOLAR ARRAY-
FULLY DEPLOYED
SIZE
J
CODE IDENT NO.
12705
DWG NO.
4045-100
SCALE 1/4
RELEASE DATE
SHEET 1 OF 1
ON
THRU
EFFECTIVE SERIAL NO.
USAGE DATA
NEXT FINAL
NEXT ASSY
USED ON
QTY REQD PER ASSY
APPLICATION
DRAWING LEVEL
H
G
F
E
D
C
B
A
16
15
14
13
12
11
10
9
8
7
6
5
4
3
2
1

Figure 27

Page intentionally left blank

Page Intentionally Left Blank

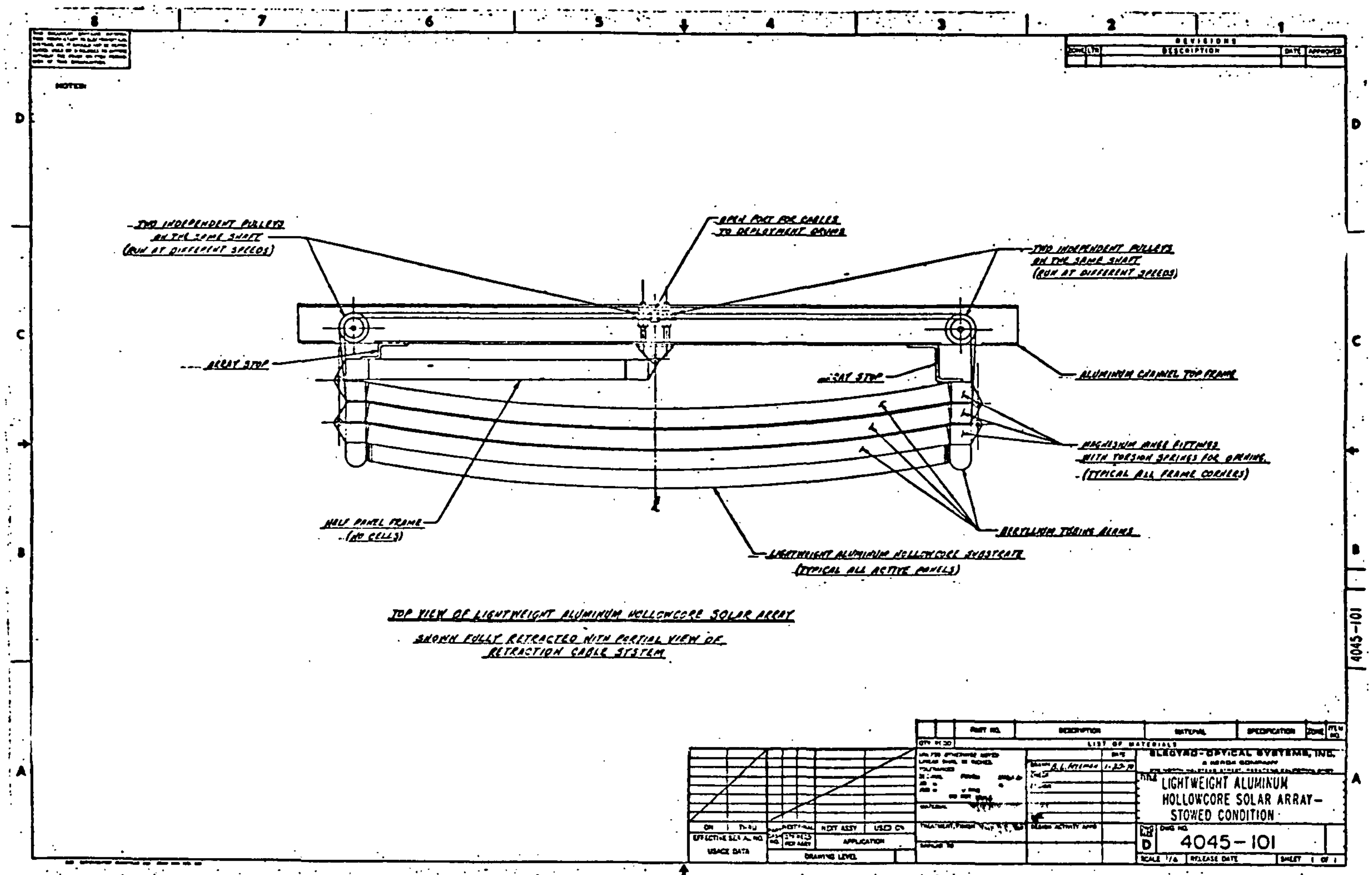
TWO INDEPENDENT PULLEYS ON THE SAME SHAFT (RUN AT DIFFERENT SPEEDS)
OPEN PORT FOR CABLES TO DEPLOYMENT DRIVE
TWO INDEPENDENT PULLEYS ON THE SAME SHAFT (RUN AT DIFFERENT SPEEDS)
ARRAY STOP
ARRAY STOP
ALUMINUM CHANNEL TOP FRAME
MAGNESIUM ANGLE FITTINGS WITH TORSION SPRINGS FOR OPENING (TYPICAL ALL FRAME CORNERS)
BERYLLIUM TUBING BEAMS
HALF PANEL FRAME (NO CELLS)
LIGHTWEIGHT ALUMINUM HOLLOWCORE SUBSTRATE (TYPICAL ALL ACTIVE PANELS)
TOP VIEW OF LIGHTWEIGHT ALUMINUM HOLLOWCORE SOLAR ARRAY
SHOWN FULLY RETRACTED WITH PARTIAL VIEW OF RETRACTION CABLE SYSTEM
ELECTRO-OPTICAL SYSTEMS, INC.
LIGHTWEIGHT ALUMINUM HOLLOWCORE SOLAR ARRAY— STOWED CONDITION
4045-101

Figure 28

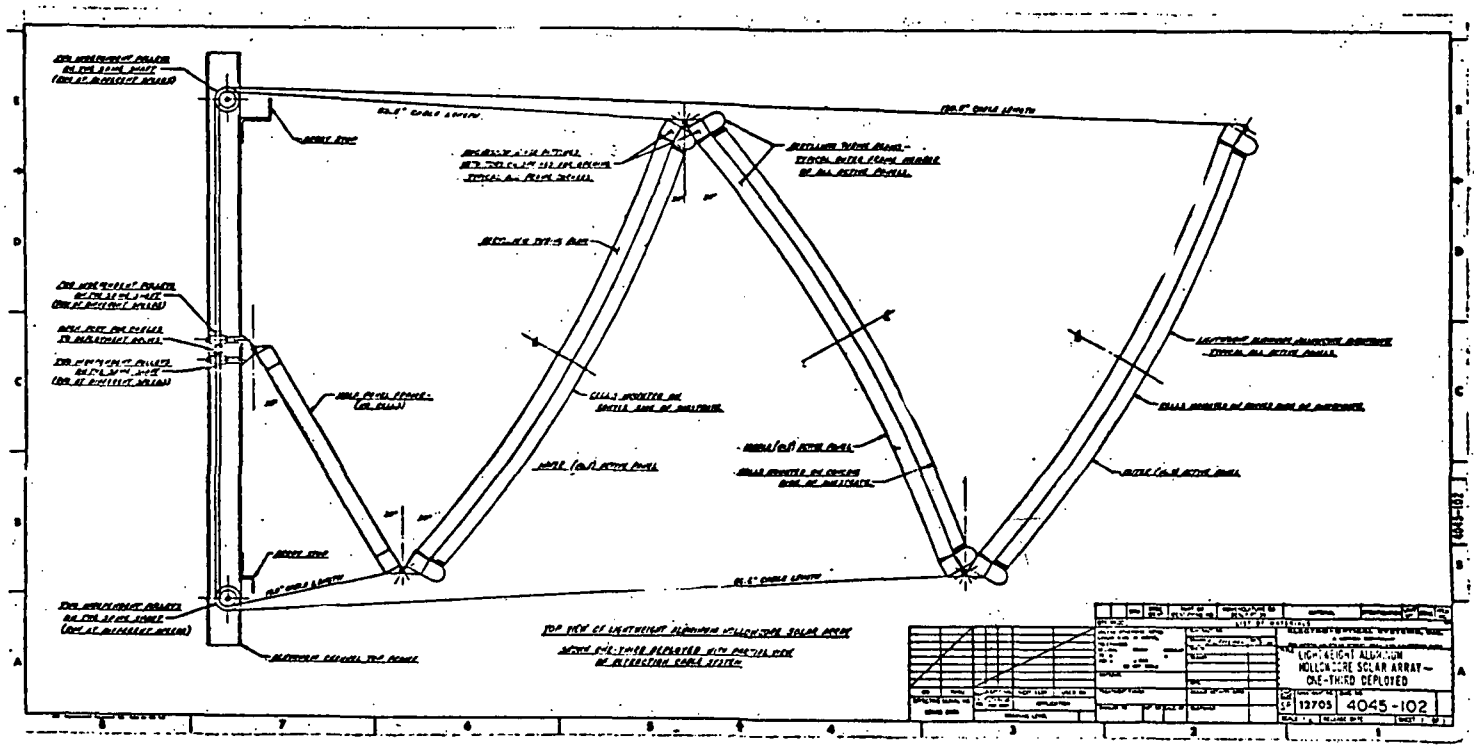
LIGHTWEIGHT ALUMINUM
HOLLOW CORE SOLAR ARRAY -
ONE-THIRD DEPLOYED
SP 12705 4045-102

Figure 29

SECTION 10

FABRICATION OF BERYLLIUM BEAMS

The four beryllium beams, EOS P/N 1121471-1, S/Ns 15, 18, 19, and 20, were completed and delivered to EOS on 22 July 1970. This work was performed by Solar Division of International Harvester, San Diego, California. These four beams will be used in the assembly of the third 5-foot by 5-foot hollowcore substrate (EOS P/N 1121477). Two units were assembled using identical beams on the previous program, Contract NAS7-428.

The eight beams fabricated on the previous program had a nominal wall thickness of 0.012 inch, on the high side of the 0.010 ±0.002 specified, and an average weight of 165 grams, with a range from 153 to 174 grams. The intent on this program was to fabricate the beam with a nominal thickness closer to 0.010 inch and reduce the weight. The weights of the four beams are:

a. S/N 15 - 144.540 grams
b. S/N 18 - 140.265 grams
c. S/N 19 - 150.682 grams
d. S/N 20 - 151.004 grams

The average weight is 146.623 grams. The total weight of the beryllium beams in the S/N 003 assembly will be 1.293 pounds compared to 1.408 pounds on S/N 001, and 1.432 pounds on S/N 002.

These beams were fabricated using the procedures and tooling described in the section titled, Fabrication of Frame Hardware in NASA Report CR 66832, "Development of Lightweight Solar Panels."

Page intentionally left blank

SECTION 11

MECHANICS OF ARRAY DEPLOYMENT

The cable deployment system will be designed to ensure that the angles between adjacent panels are equal throughout the deployment sequence. In Drawing 4045-102 (Fig. 29), the array is shown in the position where the half angle, θ, is 30° or $\pi/6$ radians. Keeping the angle between panels equal causes all panels to reach the final deployed position simultaneously and maintains control of the envelope of the swept volume.

The general relation for the cable speed as a function of the half angle, θ, and the panel angular velocity, $\dot{\theta}$, is

$$S_n = \frac{\dot{\theta} L \sin\theta \ (1 + A_n \cos\theta)}{\sqrt{2(1-\cos\theta) + A_n \sin^2\theta}}$$

where

A_1 = 0.0 (for half panel cable)
A_3 = 8.0 (for third longest cable)
A_5 = 24.0 (for second longest cable)
A_7 = 48.0 (for cable to array tip)
L = half span of panel

The cable speeds required to maintain equal θ angles with an angular constant speed, $\dot{\theta}$ = K, and with an angular speed $\dot{\theta}$ = K $\cos\theta$, are plotted in Figs. 30 and 31, respectively. A constant angular speed produces the requirement that the cable speeds are positive, and unequal at the fully deployed position, $\theta = 90^{\circ}$. An angular speed proportional to the cosine of the deployment angle, i.e., $\dot{\theta}$ = K $\cos\theta$, allows the cable speeds to

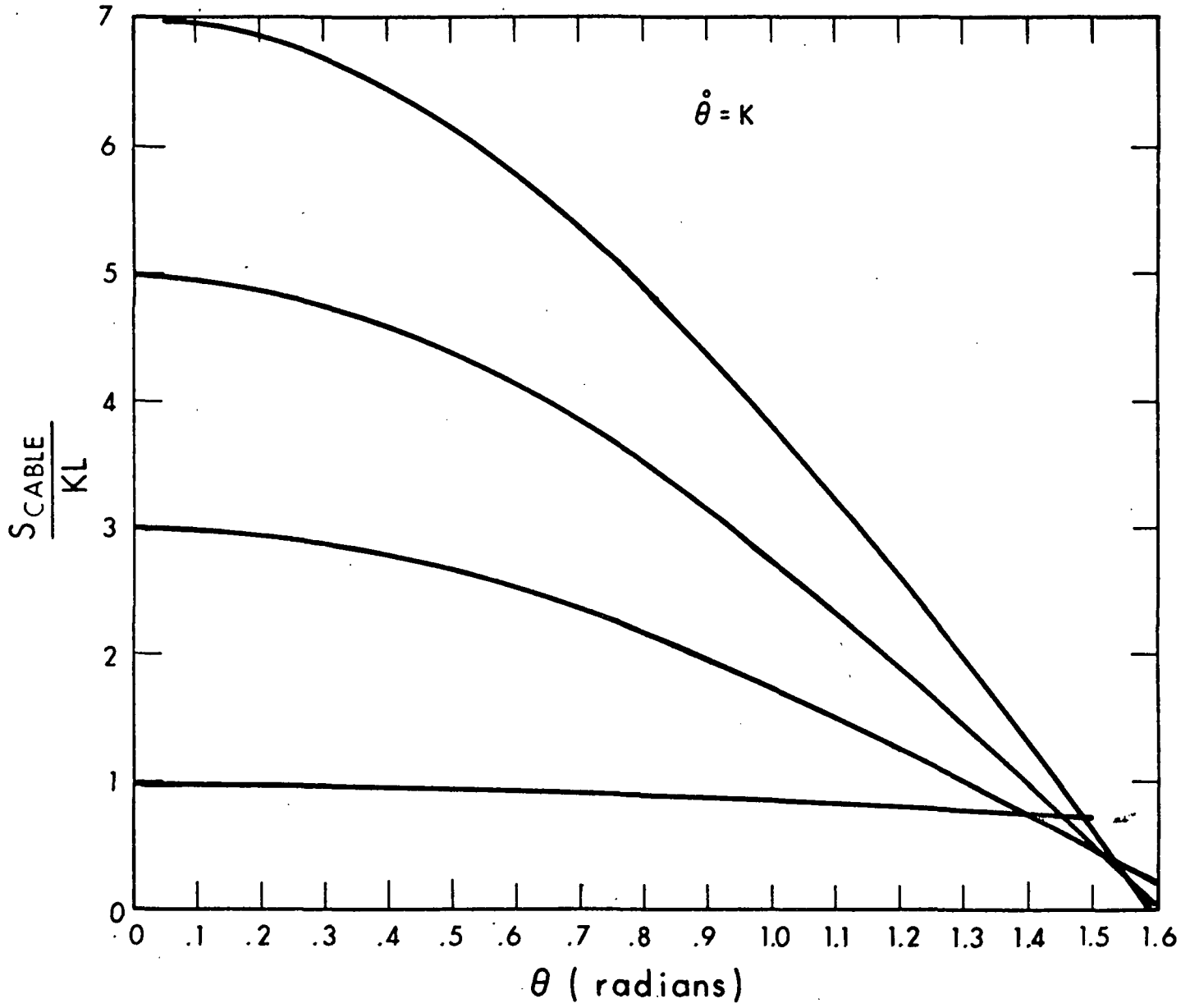

Figure 30. Cable Speed versus Deployment Angle

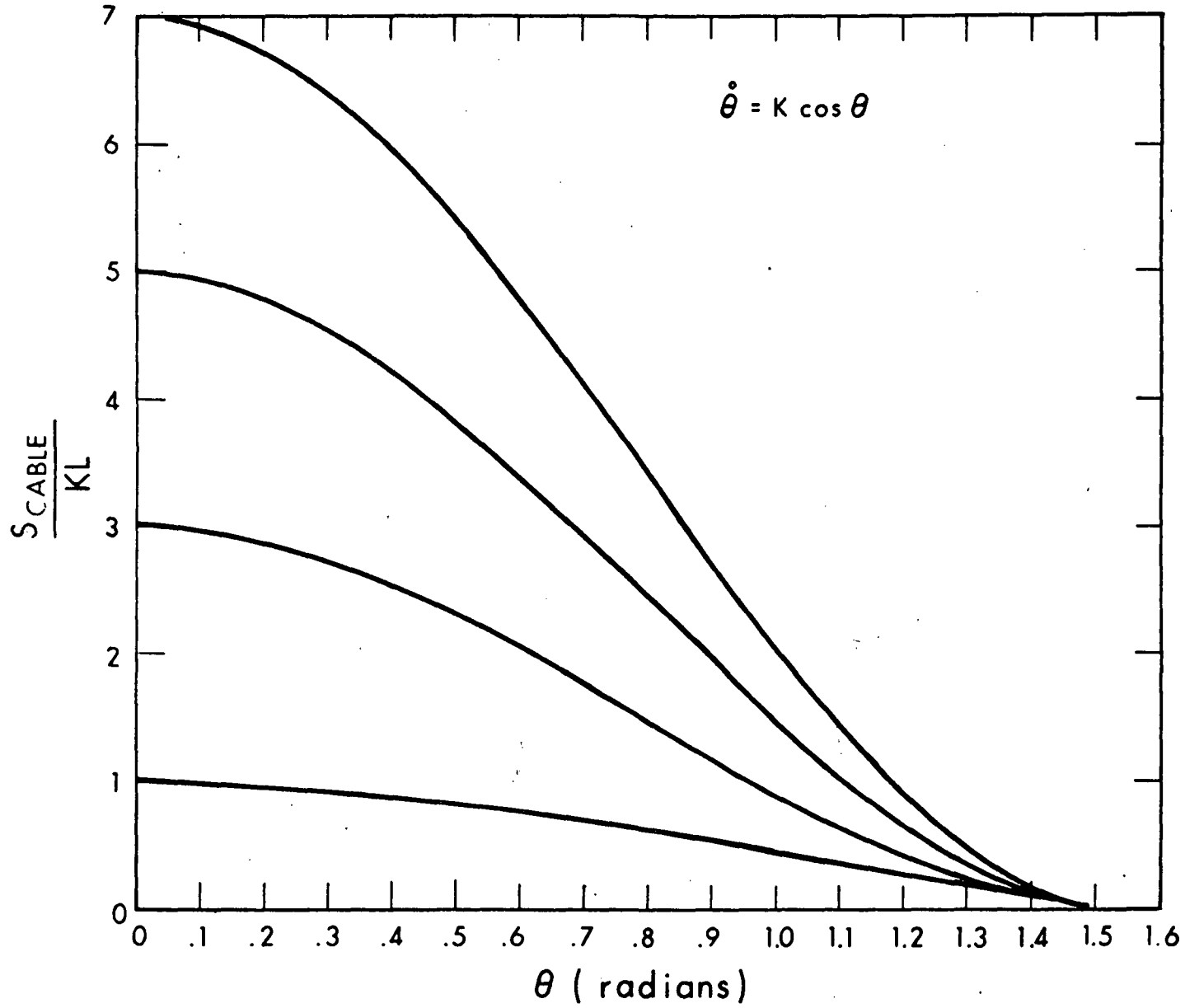

Figure 31. Cable Speed versus Deployment Angle

reach zero simultaneously at $\theta = 90^{o}$. The second approach allows the use of a single driven cable storage drum which is one of the desired design conditions.

Further investigations of the cable speed versus deployment angle relations for different angular speed functions will be performed to determine the optimum match between equipment capabilities and the performance requirements.

SECTION 12

PARAMETRIC ANALYSIS OF ALLOWABLE LOADS FOR CURVED BEAMS

12.1 DESCRIPTION

The frame, which supports the boundaries of the biconvex hollowcore substrate, utilizes tubular beryllium beams. The beams must withstand a large bending moment from a spring which deploys the panel.

Following is a parametric study with the (a) radius of curvature, (b) tube radius, (c) tube thickness, and (d) length as variables. The allowable bending moment based on yield strength and buckling criteria is calculated as a function of these variables.

12.2 STRESS ANALYSIS

The curved tubular beam is loaded with a bending moment and a shear force as shown in Fig. 32.

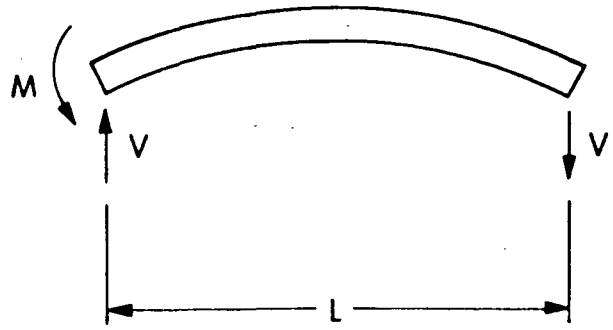

36652

Figure 32. Stress Analysis

The allowable bending moment is defined as the bending moment which produces a bending stress, σ, which has a margin of safety of zero on the material yield strength, using a factor of safety of 1.25.

When a curved beam is bent in the plane of initial curvature, plane sections remain plane; but, because of the different lengths of fibers on the inner and outer sides of the beam, the distribution of stress and strain is not linear. The neutral axis, therefore, does not pass through the centroid of the section.

The maximum bending stress in curved beams of hollow circular cross section is

$$\sigma_{MAX} = \frac{Mr}{I}\left(\frac{2}{3K\sqrt{3\beta}}\right)^{*} \qquad (1)$$

where

$$K = 1 - \frac{9}{10 + 12\ (tR/r^2)^2}$$

$$\beta = \frac{6}{5 + 6\ (tR/r^2)^2}$$

t = wall thickness, in.

R = radius of curvature of beam

= 160 in.

r = tube radius, in.

M = bending moment

$$I = 0.785\left[r^4 - (r-t)^4\right] \text{ in.}^4$$

*"Formulas for Stress and Strain," by R. J. Roark, McGraw Hill Book Company, 4th Edition.

This maximum stress does not occur at the extreme fiber, but at a distance $r\sqrt{1/3\beta}$ from the central axis. Figure 33 is a plot showing the location of the maximum stress relative to the central axis for different tube radii. The fraction, x, is the ratio of the distance from the central axis to the outer tube radius. The expression for x is

$$x = \sqrt{\frac{1}{3\beta}}$$

At x = 1.0, the shell theory and the beam theory are used. In the beam theory the maximum bending stress is

$$\sigma_{MAX} = \frac{Mr}{I} \qquad (2)$$

This maximum stress occurs at the extreme fiber of the tube.

The maximum shear stress for the hollow tube is

$$\tau_{MAX} = \frac{0.5Vr\sqrt{r^2 - y^2}}{I} \qquad (3)$$ *

where

V = M/L

L = the projected length of the beam

y = the distance of the maximum bending stress from the central axis

= $r\sqrt{1/3\beta}$

*"Engineering Design," by J. H. Faupel, John Wiley and Sons, Inc., 1964.

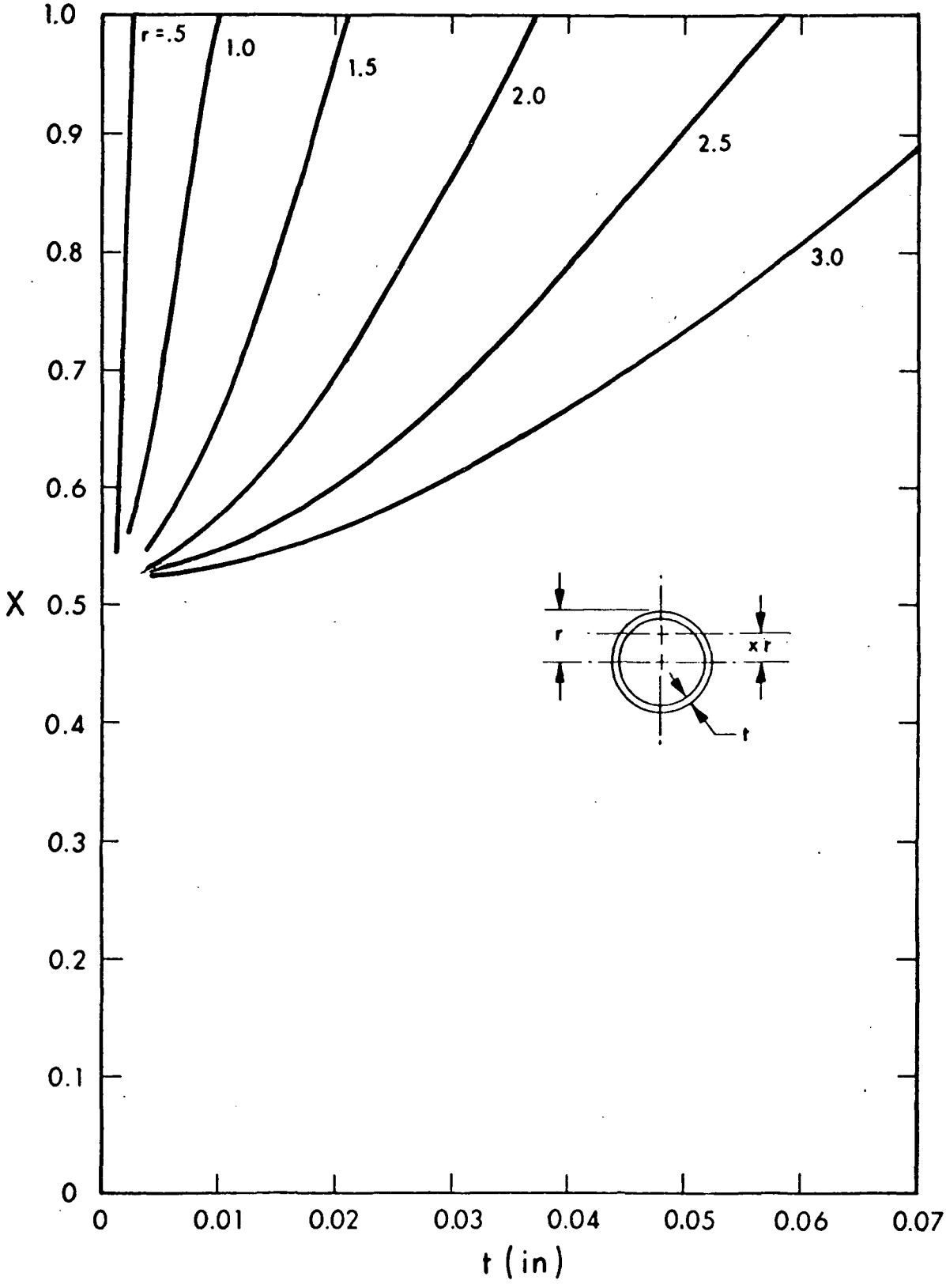

Figure 33. Location of Maximum Stress from Central Axis versus Tube Thickness

The shear stress has a parabolic distribution with a maximum value at the central axis of

$$\tau = 2V/A$$

and zero at the extreme fiber, $y = r$.

The principal bending stress of the thin wall shell is

$$\sigma^1 = \frac{\sigma_{MAX}}{2} + \sqrt{\left(\frac{\sigma_{MAX}}{2}\right)^2 + \tau_{MAX}^2}$$

substituting (1) and (3) into the above equation

$$\sigma^1 = \frac{Mr}{3IK\sqrt{3\beta}} + \sqrt{\left(\frac{Mr}{3IK\sqrt{3\beta}}\right)^2 + \left(\frac{0.5\ Mr\sqrt{r^2 - y^2}}{LI}\right)^2}$$

let

$$\sigma^1 = \sigma_y/SF$$

$$M = M_{ALLOW}$$

where

σ_y = yield strength of beryllium
= 50,000 psi

SF = safety factor = 1.25

substituting and rearranging

$$\left(\frac{0.5r\sqrt{r^2 - y^2}}{3LI}\right)^2 M_{ALLOW} + \frac{0.308\ r\sigma_y}{IK\sqrt{\beta}} M_{ALLOW} - \left(\frac{\sigma_y}{1.25}\right)^2 = 0 \qquad (4)$$

Also substituting into the beam equation (2) for the allowable bending moment, the resulting equation is

$$M_{ALLOW} = \frac{I \sigma_y}{1.25r} \qquad (5)$$

Figure 8 shows the solution of Eqs. (4) and (5) used in conjunction with Fig. 7 for the following range of variables:

a. t = 0.004 to 0.030 in.
b. r = 0.5 to 3 in.
c. L = 4, 5, 6 ft.

For r = 0.5, the beam equation (5) is used. A theory transition is made for r = 1.0 and 1.5 as denoted in Fig. 34.

12.3 STRUCTURAL STABILITY ANALYSIS

Local buckling of a curved beam is produced by the bending stress at the extreme fiber of the tube. This stress does not always represent the maximum stress, as discussed in the stress analysis.

The actual stress in the extreme fiber of the curved beam on the concave side is

$$\sigma_i = K_i \sigma^*$$

*"Formulas for Stress and Strain," by R. J. Roark, McGraw Hill Book Company, 4th Edition.

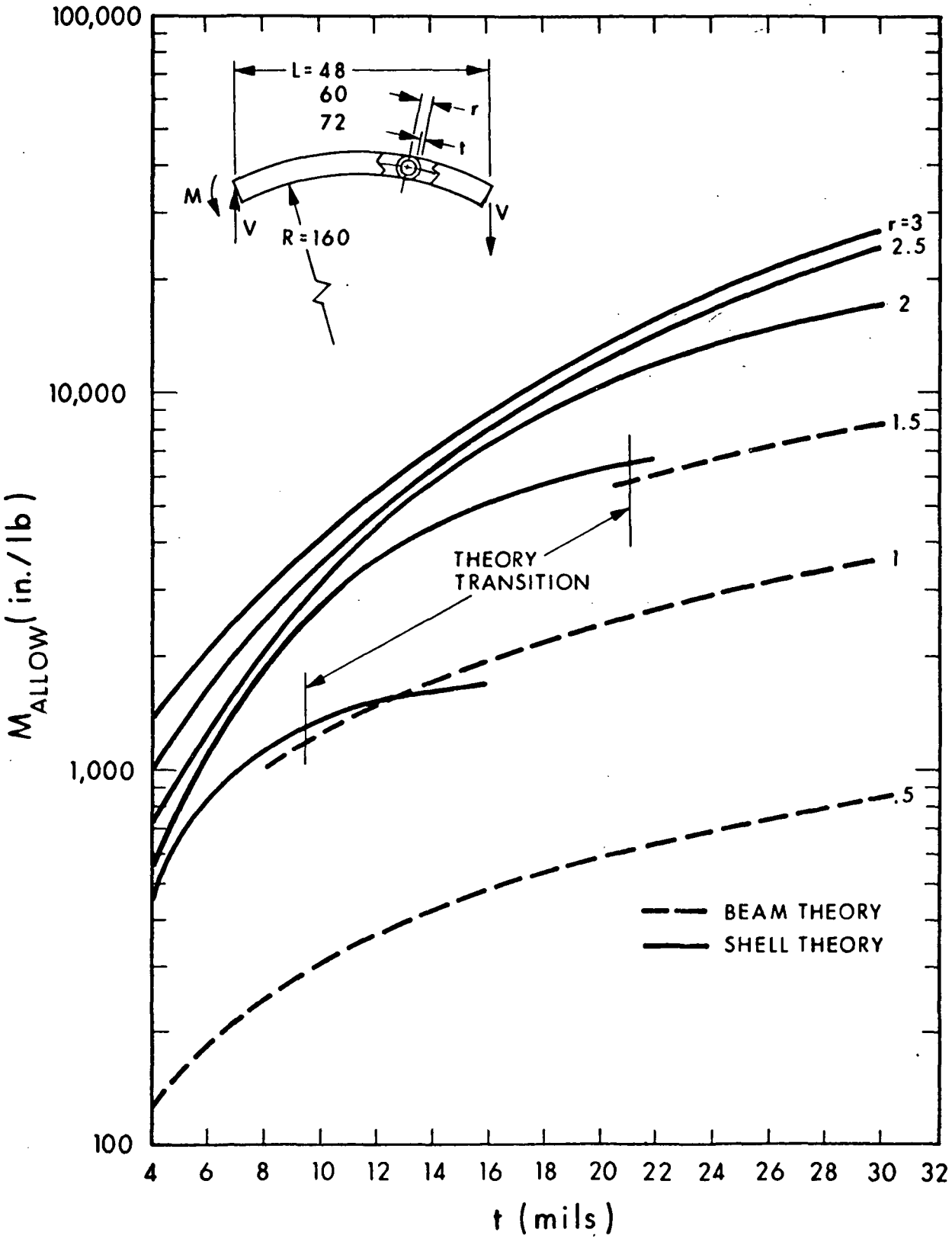

Figure 34. Allowable Bending Moment versus Wall Thickness

where

$$K_i = 1 + \frac{1.05I}{2r^3}\left[\frac{1}{R-r} + \frac{1}{R}\right]$$

$$\sigma = \frac{Mr}{I}$$

substituting

$$\sigma_i = \frac{Mr}{I}\left[1 + \frac{1.05I}{2r^3}\left(\frac{1}{R-r} + \frac{1}{R}\right)\right] \tag{6}$$

For long cylinders, the buckling stress may be determined from

$$\sigma_{CR} = 1.3\ CE\ \frac{t}{r} \tag{7}$$

*

where

E = Modulus of elasticity for beryllium
= 42.5×10^6 psi

The value of C is found in Fig. 35 with an average value of U = 0.00025, where U is the unevenness factor. The unevenness factor represents the initial imperfections of the cylinder.

Equating Eq. (6) to (7) will produce the following critical buckling moment equation:

$$\frac{M_{CR}r}{I}\left[1 + \frac{1.05I}{2r^3}\left(\frac{1}{R-r} + \frac{1}{R}\right)\right] = 1.3\ CE\ \frac{t}{r} \tag{8}$$

---

*TN3783, "Handbook of Structural Stability," Part III - Buckling of Curved Plates and Shells.

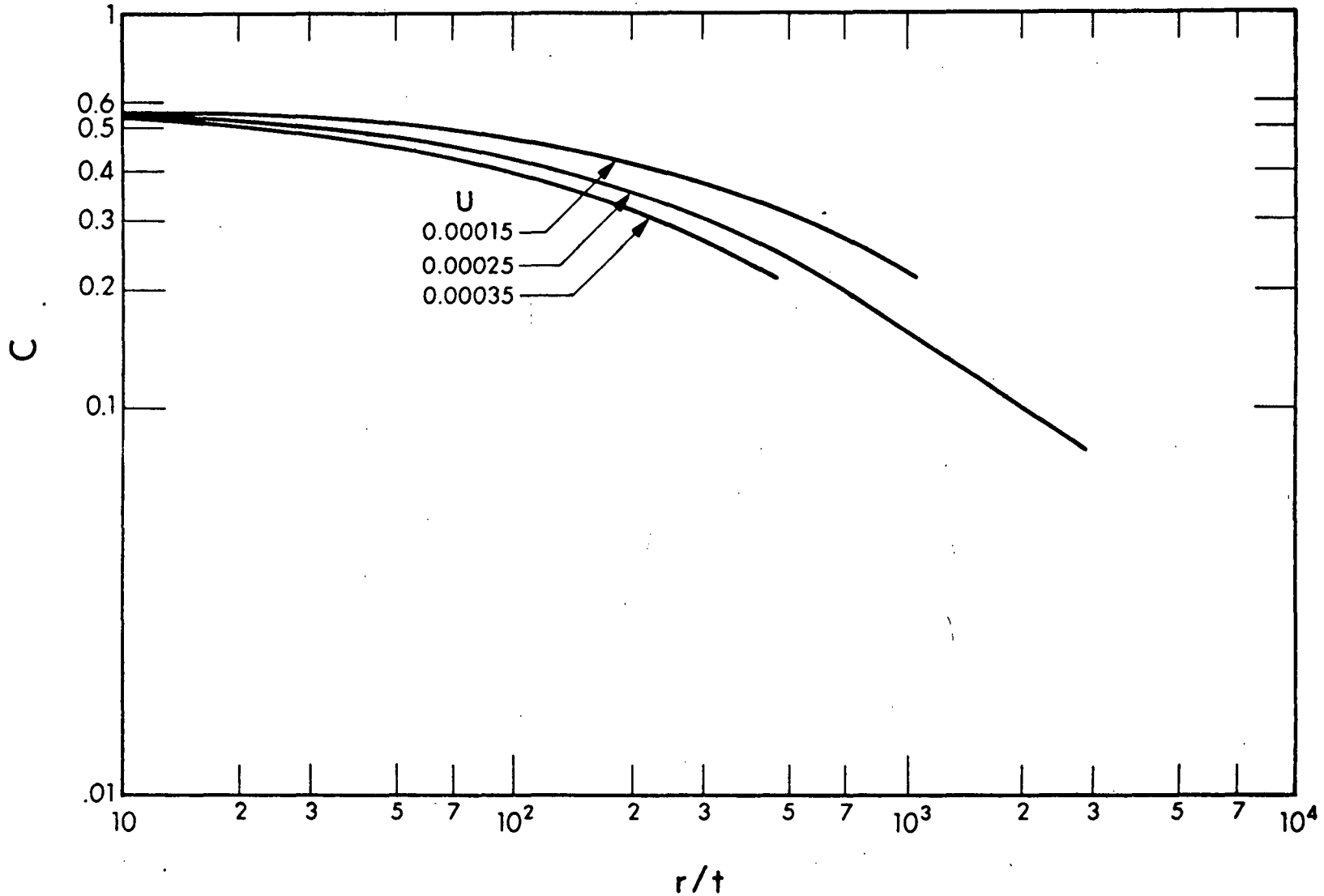

Figure 35. Modified Classical Buckling Coefficient as a Function of r/t

Figure 36 shows a plot of the buckling equation for different tube radii. The results are larger than the allowable bending moments in Fig. 34 which are based on the elastic limit. Thus, the frame for the panel is strength limited rather than stiffness or buckling limited.

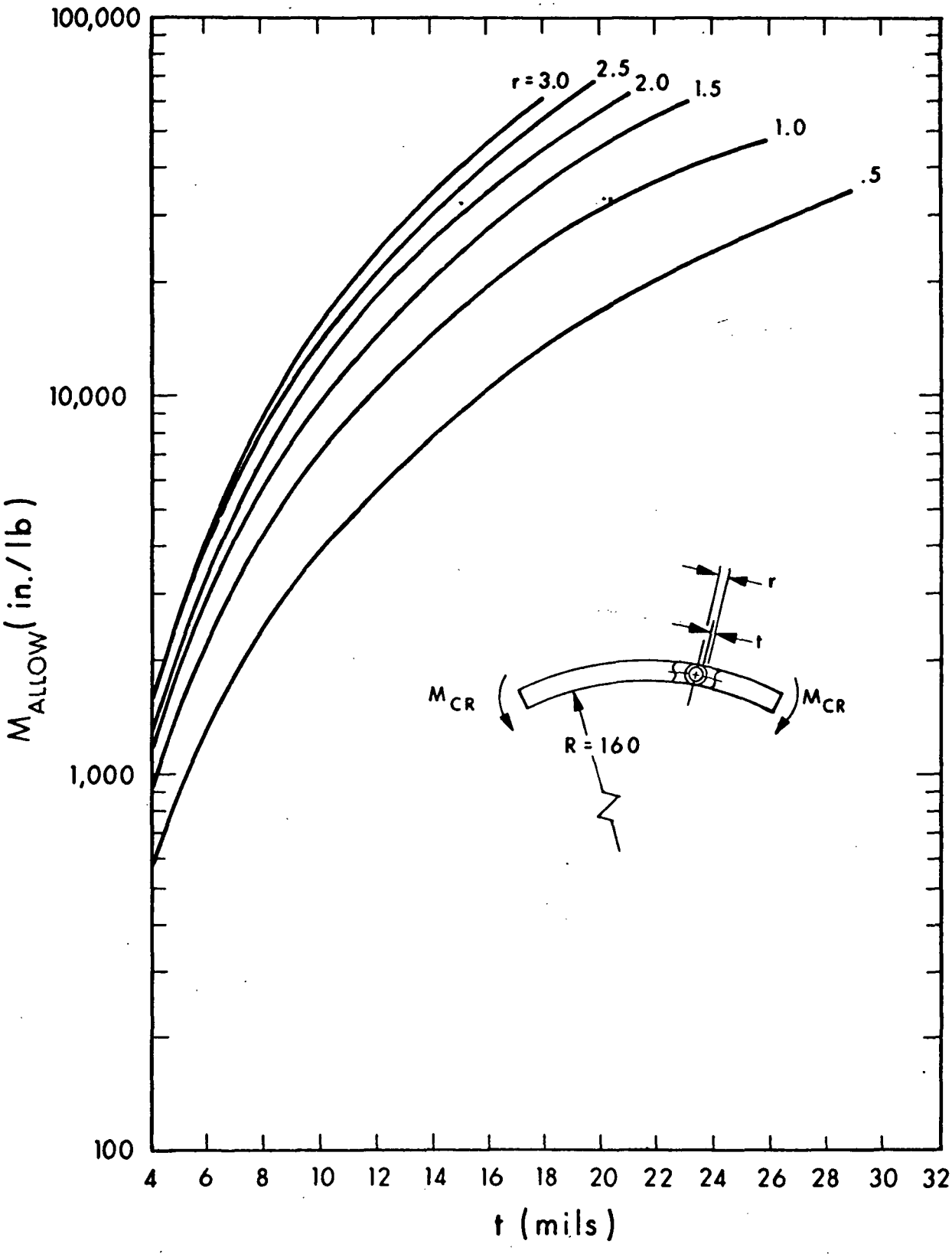

Figure 36 Critical Buckling Moment versus Wall Thickness

Page intentionally left blank

SECTION 13

CONCLUDING REMARKS AND RECOMMENDATIONS

The primary objective of the program was to develop and demonstrate the technology required for fabrication of a lightweight-deployable solar cell array. This work was an extension of technology developed under Contract NAS7-428 and reported in NASA CR-66832, Development of Lightweight Solar Panels. The following comments are considered pertinent:

a. A baseline configuration for a three-section, 75 square foot folding array with retraction capability was developed which would utilize electroformed aluminum hollowcore substrates and beryllium frames.

b. Fabrication of beryllium beams, which required considerable development in the previous contract, proceeded with little difficulty in this contract.

c. The three section array was not fabricated, demonstrated, and tested because of difficulties with impurities in the aluminum electroforming bath. These impurities, while preventing fabrication of 5 foot by 5 foot hollowcore substrates, did give ultimate tensile strengths as high as 34,000 psi.

d. From evaluation of mandrel materials for electroforming aluminum hollowcore substrates, it was concluded that a copper mandrel with nitric acid etchant is the best system to use. A procedure was developed, by varying mandrel configuration and acid concentration and temperature, for etching virtually any size aluminum hollowcore panel completely free of copper in approximately one hour.

e. From studies performed during preparation of the aluminum electroforming solution, it was concluded that in order to predict and control the material characteristics of the finished electroform, it is necessary to institute in-process check points in the solution preparation and plating procedures. Procedures were developed for evaluating peroxide content, water content, total aluminum content, and lithium-aluminum-hydride content. It is recommended that additional techniques for solution analysis be refined or developed.

f. It is recommended that the existing aluminum electroforming equipment be modified to eliminate leakage and corrosion problems, to include multiple storage and continuous filtering systems, and to include pumping systems which allow pumping with positive pressures.

g. It is recommended that purity of raw materials for the aluminum electroforming solution, particularly the aluminum chloride, be carefully controlled.

REFERENCES

1. K. E. Nelson, E. E. Luedke, and J. T. Bevans, "A Device for the Rapid Measurement of Total Emittance," J. Spacecraft Rockets 3:758-760 (1966).

2. F. S. Johnson, "The Solar Constant," J. Meterorol 11:431-439 (1954).

3. E. Schmidt and E. Eckert, "Uber die Richtungsverteilung der Warmestrahlung von Oberflachen," Forsch Gebiete Ingenieurw, 6:175-183 (1935),

   and also reproduced in

   E. R. G. Eckert and R. M. Drake, Jr., "Heat and Mass Transfer," 2nd Edition, McGraw-Hill Book Co., Inc., New York (1959).

4. J. A. Carlson, "Development of Lightweight Solar Panels," NASA CR-66832.

NASA CR-112002

DISTRIBUTION LIST
NAS1-9495

	No. Copies
NASA Langley Research Center Hampton, VA 23365	
Attn: Program Reports & Analysis Unit, Mail Stop 122	1
Raymond L. Zavasky, Mail Stop 110	1
Technology Utilization Office, Mail Stop 139A	1
Edward L. Hoffman, Mail Stop 188A	10
NASA Ames Research Center Moffett Field, CA 94035	
Attn: Library, Stop 202-3	1
Federico G. Casal, Mail Stop 202-8	1
John V. Foster, Mail Stop 200-18	1
NASA Flight Research Center P. O. Box 273 Edwards, CA 93523	
Attn: Library	1
NASA Manned Spacecraft Center 2101 Webster Seabrook Road Houston, TX 77058	
Attn: Library, Code JM6	1
Fulton Plauche, Code EP5	1
Charles Glassburn, Code EP5	1
Gene T. Rice, Code EG42	1
Jet Propulsion Laboratory 4800 Oak Grove Drive Pasadena, CA 91103	
Attn: Library, Mail 111-113	1
Donald W. Ritchie, Mail 198-220	1
Robert K. Yasui, Mail 198-220	1
John V. Goldsmith, Mail 198-220	1
NASA Marshall Space Flight Center Huntsville, AL 35812	
Attn: Library	1
Jimmy L. Miller, S&E-ASTR-EPN	1
Richard J. Boehme, PD-DO-EP	1
NASA Wallops Station Wallops Island, VA 23337	
Attn: Library	1
NASA Lewis Research Center 21000 Brookpark Road Cleveland, OH 44135	
Attn: Library, Mail Stop 60-3	1
A. F. Forestieri, Mail Stop 302-1	1
Dr. Bernard Lubarsky, Mail Stop 3-3	1

NASA CR-112002

DISTRIBUTION LIST
NAS1-9495

	No. Copies
NASA Goddard Space Flight Center Greenbelt, MD 20771	
Attn: Library	1
John W. Fairbanks, Code 716	1
William R. Cherry, Code 716	1
Luther W. Slifer, Jr., Code 716	1
Milton Schach, Code 713	1
Robert L. Weitzel, Code 481	1
NASA John F. Kennedy Space Center Kennedy Space Center, FL 32899	
Attn: Library, Code IS-DOC-12L	1
National Aeronautics & Space Administration Washington, DC 20546	
Attn: Library, Code KSS-10	1
Ernst M. Cohn, Code RPP	1
A. M. Greg Andrus, Code SCC	1
S	
Headquarters, United States Air Force Washington, DC 20330	
Attn: Major Gerald Starkey, AFRST-D	1
Wright-Patterson Air Force Base Dayton, OH 45433	
Attn: Joseph Wise	1
Dave Massie	1
George Sherman	1
NASA Scientific & Technical Information Facility P. O. Box 33 College Park, MD 20740	8 plus reproducible
Union Carbide Corporation Materials Systems Division P. O. Box 24166 Indianapolis, IN 46224	
Attn: Library	1

NASA CR-112002
National Aeronautics and Space Administration
DEVELOPMENT OF LIGHTWEIGHT ALUMINUM HOLLOWCORE SOLAR CELL ARRAY TECHNOLOGY. J. A. Carlson. December 1971.

The primary objective of the program was to develop and demonstrate the technology required for fabrication of a lightweight-deployable solar cell array. A baseline configuration for a three section folding array, with retraction capability, was developed which would utilize electroformed aluminum hollowcore substrates and beryllium frames. The three section array was not fabricated because of difficulties with impurities in the aluminum electroforming bath. A procedure was developed for etching the copper mandrel from virtually any size aluminum hollowcore panel in approximately one hour. Procedures were developed for analyzing the content of peroxide, water, total aluminum, and lithium-aluminum-hydride in an aluminum electroforming solution.

I. J. A. Carlson
II. NASA CR-112002

NASA